Cell Reports
Report

Interleukin-17D Mediates Tumor Rejection through Recruitment of Natural Killer Cells

Timothy O'Sullivan,[1] Robert Saddawi-Konefka,[1] Emilie Gross,[1] Miller Tran,[2] Stephen P. Mayfield,[2] Hiroaki Ikeda,[3] and Jack D. Bui[1,*]
[1]Department of Pathology, University of California, San Diego, 9500 Gilman Drive MC 0612, La Jolla, CA 92093, USA
[2]Department of Biology, University of California, San Diego, 9500 Gilman Drive MC 0612, La Jolla, CA 92093, USA
[3]Department of Immuno-Gene Therapy, Mie University Graduate School of Medicine, 2-174 Edobashi, Tsu, Mie 514-8507, Japan
*Correspondence: jbui@ucsd.edu
http://dx.doi.org/10.1016/j.celrep.2014.03.073

SUMMARY

The process of cancer immunoediting generates a repertoire of cancer cells that can persist in immune-competent hosts. In its most complex form, this process begins with the elimination of highly immunogenic unedited tumor cells followed by the escape of less immunogenic edited cells. Although edited tumors can release immunosuppressive factors, it is unknown whether unedited tumors produce cytokines that enhance antitumor function. Utilizing gene microarray analysis, we found the cytokine interleukin 17D (IL-17D) was highly expressed in certain unedited tumors but not in edited mouse tumor cell lines. Moreover, forced expression of IL-17D in edited tumor cells induced rejection by stimulating MCP-1 production from tumor endothelial cells, leading to the recruitment of natural killer (NK) cells. NK cells promoted M1 macrophage development and adaptive immune responses. IL-17D expression was also decreased in certain high-grade and metastatic human tumors, suggesting that it can be targeted for tumor immune therapy.

INTRODUCTION

The cancer immunoediting process involves the initial elimination of highly immunogenic tumor cells from an "unedited" heterogeneous cell repertoire, followed by the eventual escape of poorly immunogenic, "edited" cells (Schreiber et al., 2011; Shankaran et al., 2001). Edited cell lines, which are derived from tumors that develop in wild-type (WT) mice, are termed "progressors" because they are poorly immunogenic and grow progressively when transplanted into syngeneic naive WT mice. Unedited cell lines, which are derived from immune-deficient mice, are often highly immunogenic and are termed "regressors" because they are rejected when transplanted into syngeneic naive WT mice. Immune cells can infiltrate, recognize, become activated, and eliminate regressor, but not progressor, tumor cells (Bui et al., 2006; Flood et al., 1987; Shankaran et al., 2001).

Edited tumors possess antigens (Boon and van der Bruggen, 1996; DuPage et al., 2012) that can concomitantly immunize the host (Vaage, 1971), but the adaptive immune response to edited tumors ultimately fails, leading to cancer progression and death (Schreiber et al., 2011). The failure of the adaptive immune response to control antigenic tumors can involve multiple mechanisms that are intrinsic to the tumor cell, including antigen loss and acquisition of inhibitory ligands, or tumor-cell-extrinsic effects, including immune suppressive cytokines and antigen tolerance (Schreiber et al., 2011; Zitvogel et al., 2006; Zou and Chen, 2008). It is not known to what extent tumor-extrinsic effects or intrinsic escape mechanisms contribute to cancer progression. Nevertheless, it is clear that progressor tumors express cytokines such as transforming growth factor β (TGF-β) that can inhibit antitumor immune responses (Bierie and Moses, 2010). In contrast, it has not been shown whether regressor cells can produce cytokines that serve to activate antitumor immunity. Importantly, cytokine-based immune therapy is a mainstay for treatment of human cancers such as melanoma and renal cell carcinoma (Nicholas and Lesinski, 2011; Rosenblatt and McDermott, 2011). In these diseases, treatment with interleukin-2 (IL-2) and interferon α (IFNα) is associated with severe toxic effects that limit therapeutic efficacy (Garbe et al., 2011; Hutson, 2011). Thus, discovering novel, safe, nontoxic cytokines that can mediate tumor rejection would have a high impact on tumor immune therapy.

The IL-17 family of cytokines is one of the most ancient cytokine families (Paul, 2013) and includes six members (IL-17A, IL-17B, IL-17C, IL-17D, IL-17E, and IL-17F) identified by homology that possess a putative cysteine-knot structure (Iwakura et al., 2011; Kolls and Lindén, 2004). IL-17A and IL-17F are defining members of the family and are produced by Th-17 cells to mediate immunity against extracellular bacteria and fungi. Recently, IL-17C was shown to have similar activity as IL-17A/IL-17F, although it is expressed by infected epithelial cells and not by T cells (Ramirez-Carrozzi et al., 2011; Song et al., 2011). IL-17D is a cytokine whose function is not well described, although similar to IL-17C, it is known to be expressed outside the immune system and can stimulate human umbilical vein endothelial cells to produce interleukin-6, interleukin-8 (IL-8), and granulocyte-macrophage colony-stimulating factor (GM-CSF) (Starnes et al., 2002). It has also been found in rheumatoid

nodules (Müller and Lamprecht, 2008) and is decreased in psoriatic skin (Johansen et al., 2009). Interestingly, IL-17D is considered to be the most ancient cytokine in the IL-17D family (Paul, 2013; Roberts et al., 2008), although there have been no studies addressing the function of IL-17D in cancer or any other disease model system.

In this study, we sought to identify tumor-secreted molecules that can mediate tumor rejection. We found that IL-17D is expressed in some regressor, but not in progressor, cell lines. Importantly, IL-17D is sufficient to induce rejection or growth delay when overexpressed in some progressor cells. We show that the mechanism of action of IL-17D is to stimulate production of monocyte chemotactic protein-1 (MCP-1, aka CCL2), which recruits natural killer (NK) cells to the tumor and leads to M1 macrophage development and productive antitumor adaptive immune responses. These observations identify IL-17D as a cytokine that can promote immune responses via recruitment of NK cells.

RESULTS

IL-17D Is Highly Expressed by Certain Regressor, but Not Progressor, Tumors

To identify genes that could induce tumor rejection, we used a model system whereby edited progressors and unedited regressor methylcholanthrene (MCA)-induced sarcoma cell lines were derived from syngeneic WT and immune-deficient mice (Shankaran et al., 2001; O'Sullivan et al., 2012). We performed gene microarray studies on eight regressor and 16 progressor cell lines (Figure S1A). Among the many gene expression differences detected, we focused on the cytokine IL-17D due to its unknown function in tumor biology. We found that IL-17D was highly upregulated in some regressors but was not expressed in any progressor tumor cell line tested by microarray (Figure 1A), quantitative RT-PCR (qRT-PCR) (Figures 1B and S1B), and intracellular fluorescence-activated cell sorting (FACS) and verified with an independent set of regressors/progressors from another strain (Figures S1C and S1D) (O'Sullivan et al., 2012; Shankaran et al., 2001). Furthermore, treatment of regressor tumor cell lines with protein transport inhibitors doubled the amount of intracellular IL-17D signal (Figure 1C), confirming its secretion.

To assess the expression of *IL-17D* in human cancers, we utilized publicly available National Center for Biotechnology Information (NCBI) Gene Expression Omnibus (GEO) data sets to examine *IL-17D* expression in multiple malignant human tissues. Interestingly, *IL-17D* gene expression was decreased in metastatic prostate tumors compared to primary prostate tumors (Figure 1D) and was also suppressed in more advanced, higher-stage gliomas (World Health Organization [WHO] grade III astrocytoma, grade IV glioblastoma multiforme [GBM]) relative to less advanced, lower-stage gliomas (WHO grade II oligodendroglioma) (Figure 1E, left panel). Additional studies confirmed that *IL-17D* expression was suppressed in grade IV GBM when compared to grade III astrocytomas (Figure 1E, right panel) and that high expression of *IL-17D* in tumor biopsy specimens correlated with a greater survival time for a subset of patients with grade IV GBM (Figure 1F).

IL-17D Promotes Progressor Tumor Rejection but Is Not Required for Regressor Tumor Rejection

We then explored whether manipulating IL-17D expression could influence tumor growth. IL-17D was silenced in regressor cell lines by 95%–100% and overexpressed in progressors at approximately 5-fold of control cells, a level similar to the expression in unmanipulated regressors (Figures S2A–S2D). Silencing of IL-17D in regressor tumors led to a slight growth increase and delayed rejection in one regressor tumor (d42m1) while having no measurable effect in another regressor tumor (d30m4) (Figure 2A). In four of the six progressor cell lines tested, the overexpression of IL-17D led to complete rejection (F244 and d30m1) or a significant delay in growth (B16.OVA and LLC) in WT mice (Figure 2B). This effect of IL-17D was due to adaptive immune cells, because in vitro and in vivo growth kinetics (in RAG2$^{-/-}$ mice) remained unchanged (Figures S2F and S2G).

To demonstrate the antitumor efficacy of IL-17D on pre-established tumors, we generated a progressor tumor cell line (F244TR17D) that expressed IL-17D upon administration of doxycycline (Figure S2E). Induced expression of IL-17D caused the rejection of 25 mm^2 tumors, but not 100 mm^2 tumors (Figure 2C), indicating IL-17D was most effective in inducing rejection of small tumors. We then tested whether intratumoral injections of recombinant IL-17D could mediate tumor regression of pre-established B16.OVA tumors transplanted into WT mice. Strikingly, intratumoral injections of recombinant IL-17D caused a significant growth delay compared to control-treated tumors, demonstrating the antitumor efficacy of IL-17D (Figure 2D).

IL-17D Expression Enhances Recruitment of NK Cells in Progressor and Regressor Tumors

To define the mechanism of IL-17D-mediated tumor rejection, we characterized tumor-infiltrating immune cells in tumors with high and low levels of IL-17D. We found an approximately 2-fold increase in the amount of NK cells in tumors with high versus low IL-17D (Figures 3A and 3B). These NK cells had similar phenotype to splenic NK cells and did not display markers found in immunoablative NK cells (Terme et al., 2012) or interferon-producing killer dendritic cells (Bonmort et al., 2008) (Figure S3). Notably, NK cells were required for tumor rejection, because mice treated with anti-NK1.1, but not control immunoglobulin G (IgG), failed to reject the IL-17D-overexpressing tumors (d30m1, F244) or showed increased growth (B16.OVA) (Figure 3C). The recruitment of NK cells likely mediates IL-17D's antitumor activity, as we did not observe enhanced numbers of either neutrophils or monocytes in tumors expressing high versus low levels of IL-17D and neutrophils were not required for IL-17D-mediated tumor rejection (data not shown).

Because it is known that NK-dependent tumor rejection can lead to priming of adaptive immune responses (Diefenbach et al., 2001; Kelly et al., 2002), we then tested whether mice that had rejected IL-17D-overexpressing tumors could reject a rechallenge with untransduced progressor tumors. Indeed, we found that parental cells were rejected in primed mice (Figure 3C), confirming that edited tumors possess antigens and that initiating the "correct" innate cell response (via IL-17D) can result in productive antigen-specific antitumor responses.

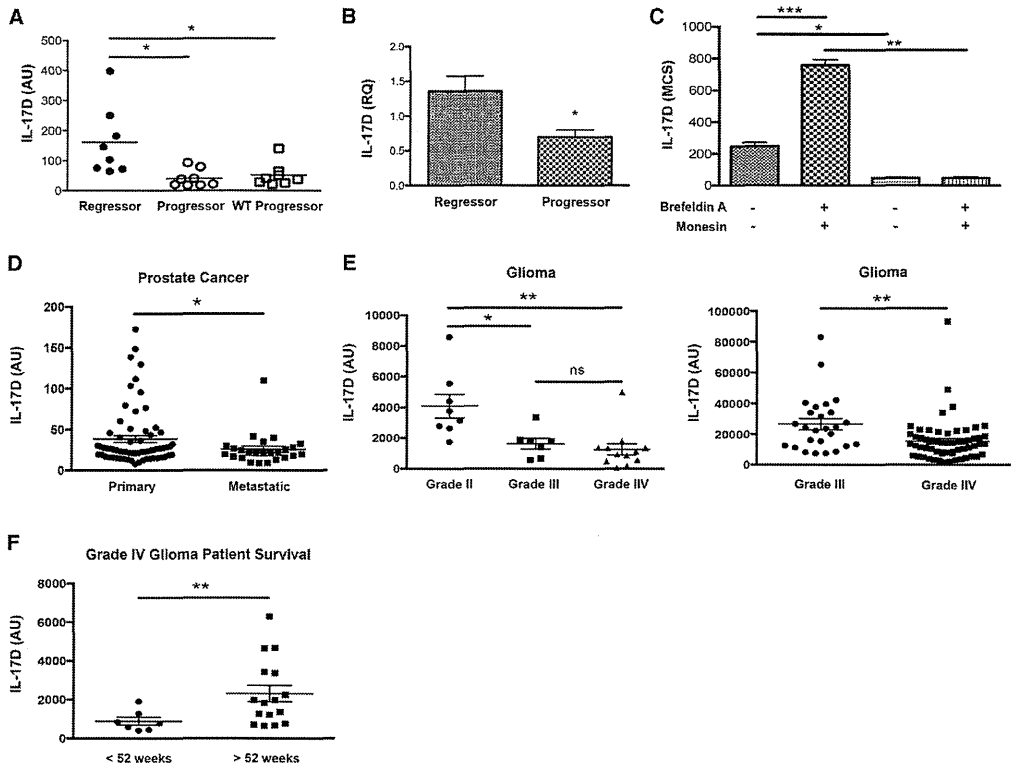

Figure 1. IL-17D Is Highly Expressed in Some Regressor Cell Lines and Is Downregulated in Progressor Tumor Cell Lines and Several Human Cancer Samples

(A) Plotted microarray data of *IL-17D* gene expression of regressor (n = 8) and progressor (n = 16) tumor cell lines.

(B) qRT-PCR analysis of independent regressor (n = 4) and progressor (n = 4) tumor cell lines.

(C) Quantitated IL-17D intracellular protein expression of 129/Sv RAG2$^{-/-}$-derived regressor (n = 3) and progressor (n = 3) tumor cell lines incubated with or without brefeldin A and monensin. IL-17D mean channel shift (MCS) values are calculated by taking the mean florescence of IL-17D intracellular protein signal and subtracting the mean fluorescence signal of the isotype control stain for the same tumor cell line sample.

(D and E) *IL17D* gene expression was evaluated from publicly available NCBI Gene Expression Omnibus data sets (GDS) from studies comparing indicated cancerous and metastatic tissue from human patients.

(F) GDS1816 samples from patients who had been diagnosed with WHO grade IV astrocytomas with necrosis were divided into low or high survival time categories, and *IL17D* gene expression was evaluated. Each point represents an individual patient sample.

Data from (B) and (C) are representative of two independent experiments. Samples were compared using an unpaired, two-tailed Student's t test with Welch's correction. Error bars are depicted as ±SEM (*$p < 0.05$, **$p < 0.01$, ***$p < 0.001$; NS, not significant).

See also Figure S1.

Previously, we have found a requirement for NK cells and interferon γ (IFNγ) in the accumulation of M1 macrophages in regressor tumors during cancer immunoediting (O'Sullivan et al., 2012). We also observed an approximately 1.5-fold enhancement in the accumulation of M1 macrophages in progressor tumors overexpressing IL-17D (Figure 3D), whereas silencing of IL-17D in regressor tumors reduced M1 macrophages by approximately 2-fold in both WT and RAG2$^{-/-}$, but not RAG2$^{-/-}$ × γc$^{-/-}$, hosts, which are deficient in NK cells (Figure 3D).

IL-17D Recruits Innate Immune Cells in an Air Pouch Model of Inflammation

To show directly whether IL-17D can induce the recruitment of immune cells, we used an in vivo air pouch model of inflammation in WT mice. Sterile air pouches become well vascularized after a period of 7 days (data not shown) and recruit immune cells rapidly after administration of lipopolysaccharide (LPS) (Pelletier et al., 2004). Indeed, we found that LPS, IL-17A, and IL-17D significantly recruited CD45^{+} immune cells into air pouches compared to PBS control (Figure 4A). When we examined the composition of the immune cells, we found that LPS and IL-17A recruited more neutrophils than any other cell type, whereas neutrophils constituted a smaller percentage of cells recruited by IL-17D (Figure 4B). Interestingly, IL-17D recruited significantly more NK cells (Figure 4C), but not monocytes (Figure 4C), neutrophils, or macrophages (Figure S4A), compared to LPS and IL-17A. We found that the IL-17D-recruited NK cells were mostly CD27^{high} (Figure S4B), which could be a semimature population

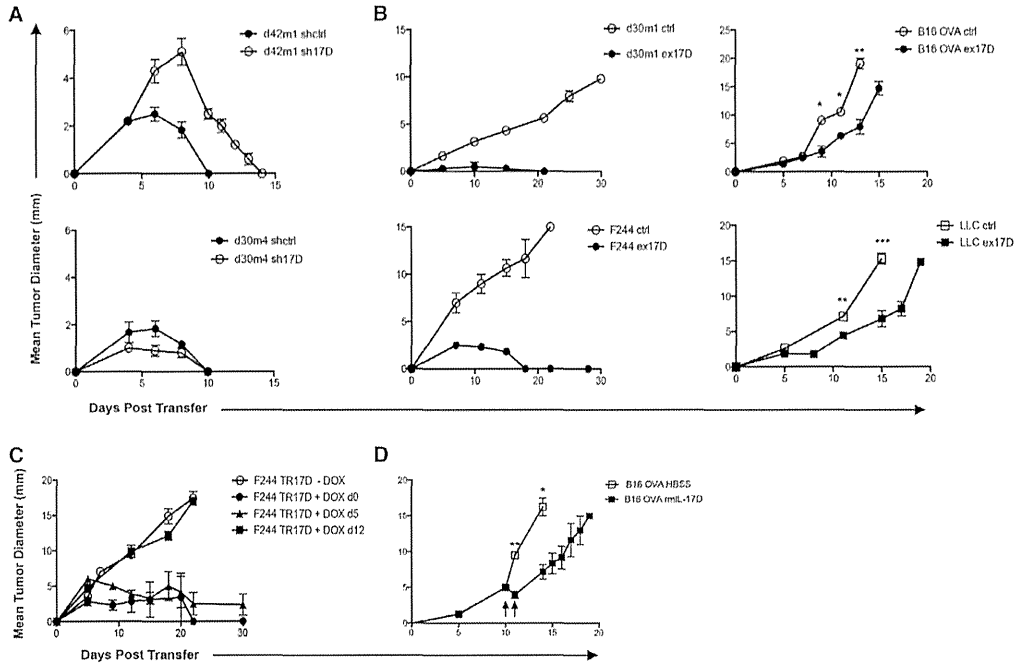

Figure 2. Expression of IL-17D Mediates Progressor Tumor Rejection

(A) Tumor growth of indicated (ctrl, sh17D) regressor tumors transplanted into WT mice (n = 5 for each tumor cell line).

(B) Tumor growth of indicated (ctrl, ex17D) progressor tumors transplanted into WT mice (n = 5 for each tumor cell line).

(C) Tumor growth of inducible IL-17D progressor tumor cell line transplanted into WT mice receiving water or doxycycline continuously from day 0 (n = 5), day 5 (n = 5), or day 12 (n = 5).

(D) Tumor growth of B16.OVA melanoma tumor cell line transplanted into WT mice and receiving intratumoral injections of IL-17D (2 μg) or Hank's balanced salt solution on days 10 and 11. Data from (A)–(D) are representative of two independent experiments. Samples were compared using an unpaired, two-tailed Student's t test with Welch's correction. Error bars are depicted as ±SEM (*$p < 0.05$, **$p < 0.01$, ***$p < 0.001$).

See also Figure S2.

of NK cells that may participate in IFNγ-dependent T cell priming in lymph nodes (Martin-Fontecha et al., 2004; Watt et al., 2008). Interestingly, IL-17D recruited approximately twice the amount of $CD27^{high}CD11b^{low}$ NK cells as LPS, with no significant recruitment of mature $CD27^{lo}$ NK cells (Figure 4D).

IL-17D Indirectly Recruits NK Cells In Vivo by Stimulating the Production of MCP-1

Because IL-17A is known to induce IL-8 from endothelial cells to recruit neutrophils (Roussel et al., 2010), we examined whether IL-17D utilized a similar mechanism. Indeed, we found that IL-17D induced the expression of MCP-1 in mouse air pouch lavage fluid (Figure 5A). We then repeated air pouch experiments in the presence of blocking antibodies specific for MCP-1 and found that anti-MCP1, but not control IgG, completely inhibited IL-17D-mediated recruitment of NK cells (Figure 5B), monocytes, and neutrophils (Figure S5A). Furthermore, qRT-PCR analysis of purified tumor endothelial cells from two IL-17D-overexpressing tumors (Figure S5B) showed a 4–17 times increase in MCP-1 transcript compared to control tumors, respectively (Figure 5C), while maintaining similar levels of VEGFR1 (Figure S5C). Notably, depletion of MCP-1 led to increased growth of two IL-17D-overexpressing tumors (Figure 5D). These results were likely due to reduced overall numbers of infiltrating NK cells, as MCP-1 depletion reduced the density of tumor-infiltrating NK cells compared to control depletion in tumors overexpressing IL-17D (Figure 5E).

DISCUSSION

The IL-17 family of cytokines promotes immune responses by inducing the expression of proinflammatory cytokines and chemokines, leading to recruitment of neutrophils and other innate immune cells (Pappu et al., 2011). IL-17A and IL-17F are produced by Th-17 cells and are involved in autoimmune disease and host responses to tissue infection. IL-17C may have similar inflammatory functions to IL-17A and IL-17F, although IL-17C is expressed in epithelial cells and is induced by microbial ligands. Our discovery that IL-17D is expressed outside the immune system and functions to recruit NK cells suggests that the IL-17 family may have evolved to evoke distinct arms of the immune response, presumably to deal with specific pathogen insults. We speculate that similar to IL-17C, the expression of IL-17D in nonimmune tissues may represent an early evolutionary adaptation to mediate local antiviral immunity through the recruitment

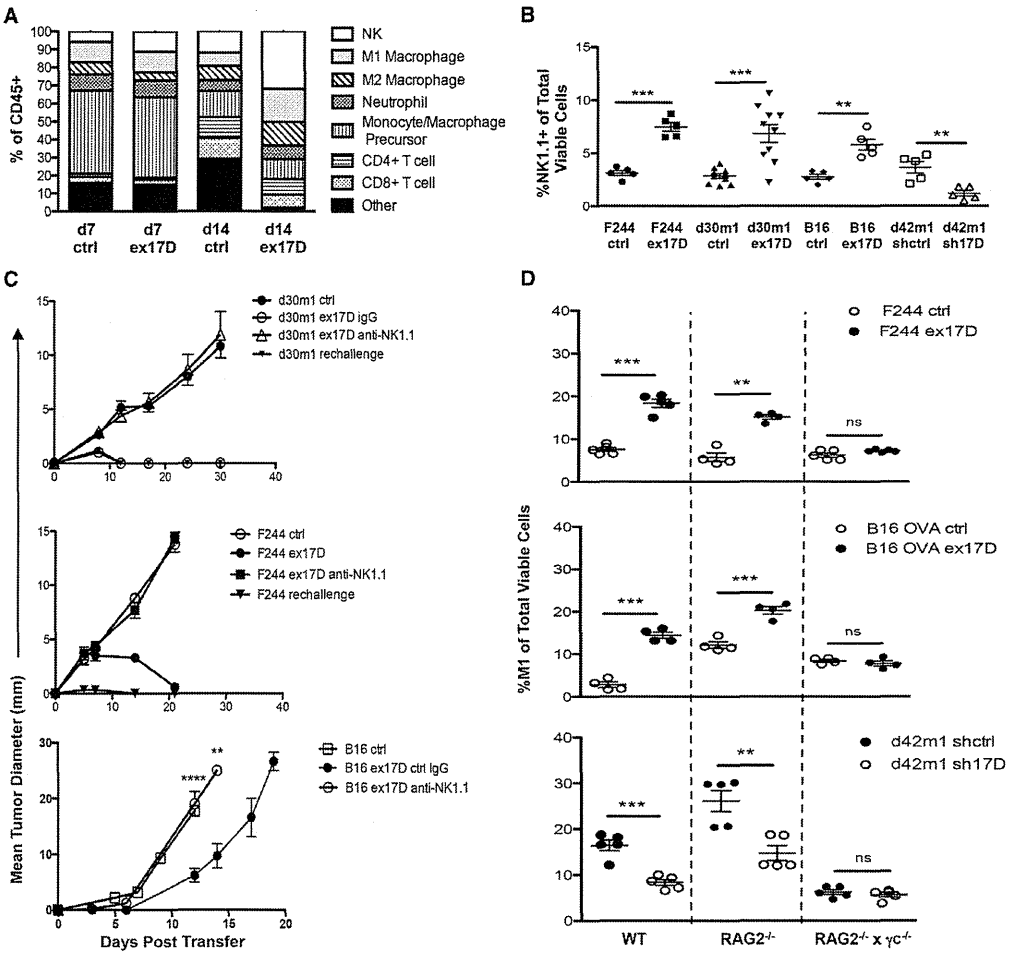

Figure 3. Overexpression of IL-17D in Progressor Tumors Recruits NK Cells that Are Required for Tumor Rejection in WT Mice and Promote M1 Macrophage Infiltration

(A) Percentage of (7AAD$^-$, CD45$^+$, CD3$^-$, NK1.1$^+$) NK cells, (7AAD$^-$, CD45$^+$, CD11b$^+$, Ly6G$^+$, MHCII^{lo}) neutrophils, (7AAD$^-$, CD45$^+$, CD11b$^+$, Ly6C^{hi}) monocytes/macrophage precursors, (7AAD$^-$, CD45$^+$, F4/80$^+$, Ly6C^{lo}, MHCII^{hi}, CD206^{lo}) M1 macrophages, (7AAD$^-$, CD45$^+$, F4/80$^+$, Ly6C^{lo}, MHCII^{lo}, CD206^{hi}) M2 macrophages, (7AAD$^-$, CD45$^+$, CD3$^+$, CD4$^+$, CD8$^-$) CD4$^+$ T cells, and (7AAD$^-$, CD45$^+$, CD3$^+$, CD4$^-$, CD8$^+$) CD8$^+$ T cell-infiltrating immune cells in F244 ctrl or ex17D tumors on days 7 and 14 posttransplantation in WT mice. ("Other" indicates infiltrating Ly6C$^-$MHCII$^-$NK1.1$^-$CD3$^-$ immune cells).

(B) Percent infiltrating NK cells of total viable (7AAD$^-$) cells from transduced regressor and progressor tumors on day 7 posttumor transplant in WT mice.

(C) Tumor growth of IL-17D overexpressing (ex17D) progressor tumors transplanted into WT mice receiving either intraperitoneal injections of anti-NK1.1/control IgG or preimmunized with transplantation of IL-17D overexpressing (ex17D) tumor cell lines.

(D) Percentage of M1 macrophages of total viable cells on day 14 posttumor transplant of progressor tumor cell lines into WT, RAG2$^{-/-}$, or RAG2$^{-/-}$ × γc$^{-/-}$ hosts.

Data from (A)–(D) are representative of two independent experiments. Samples were compared using an unpaired, two-tailed Student's t test with Welch's correction. Error bars are depicted as ±SEM (**p < 0.01, ***p < 0.001, ****p < 0.0001; NS, not significant). See also Figure S3.

of NK cells. Notably, our preliminary studies indeed have found increased IL-17D transcripts in virus-infected skin (R.S.K. and J.D.B., unpublished data). Future studies on the endogenous role of IL-17D in the context of infection, autoimmunity, and cancer and its regulation are certainly warranted.

Our studies have shown that IL-17D is poorly expressed in cancer cells that grow progressively (mouse MCA-induced sarcomas and certain human cancers) but, comparatively, can be more highly expressed in certain immunogenic MCA-induced sarcoma cells and in low-stage tumors. It is not clear what regulates the constitutive expression of IL-17D in certain cells, but it is clear that high expression of IL-17D may not be compatible with tumor progression, because advanced-stage human and edited mouse cancer cells have lower levels of IL-17D and the ectopic expression of IL-17D in progressor cells led to NK dependent tumor rejection. Overexpression of immune-cell-derived

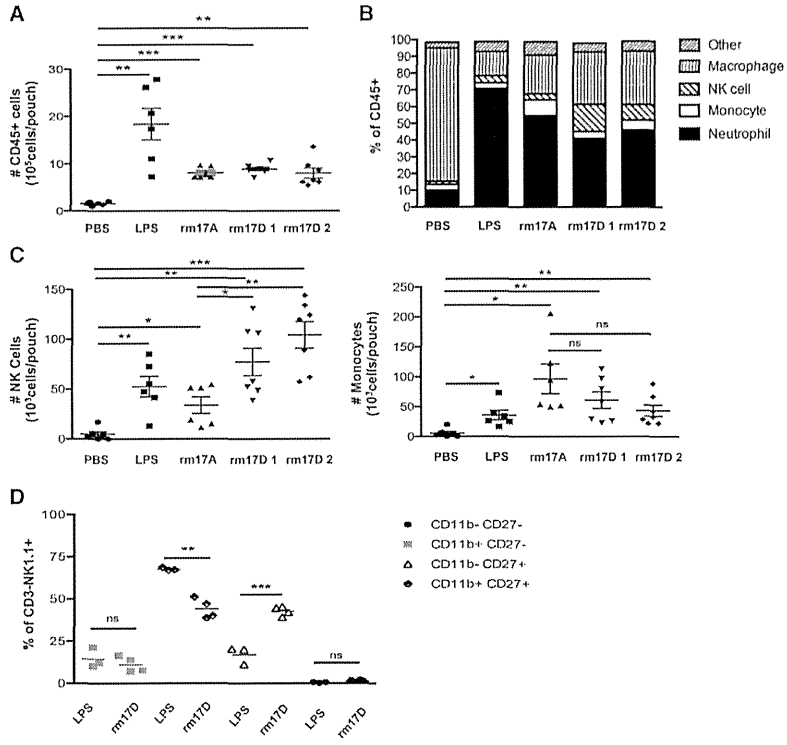

Figure 4. Recombinant Mouse IL-17D Recruits NK Cells in an Air Pouch Inflammation Model

(A) Total number of infiltrating immune cells per air pouch in WT mice receiving intrapouch injections of PBS, LPS, IL-17A, IL-17D-1 (generated from *E. coli*.), or IL17D-2 (generated from *C. reinhardtii*).

(B) Percentages of NK cells, monocytes, neutrophils, and macrophages per air pouch receiving indicated intrapouch injections. (Other indicates $CD4^+$, $CD8^+$ T cells or $Ly6C^-MHCII^-NK1.1^-CD3^-$ recruited immune cells). Cell populations are defined as in Figure 3A.

(C) Total number of NK cells and monocytes per air pouch receiving indicated intrapouch injections.

(D) Immunophenotypic analysis of infiltrating $NK1.1^+CD3^-$ NK cells in mouse air pouches receiving intrapouch injections of LPS or rmIL-17D. Data from (A)–(D) are representative of two independent experiments. Each point represents an individual mouse. Samples were compared using an unpaired, two-tailed Student's t test with Welch's correction. Error bars are depicted as ±SEM (*$p < 0.05$, **$p < 0.01$, ***$p < 0.001$). See also Figure S4.

chemokines and cytokines such as GM-CSF (Dranoff, 2004; Dranoff et al., 1993) and IL-15 (Liu et al., 2012) have already been demonstrated to have potent antitumor efficacy. Our findings are unique in that IL-17D is tumor expressed (rather than immune cell derived) and thus likely represents an endogenous tumor surveillance activity.

It should be noted that not all regressors have high levels of IL-17D (Figure 1) and that there are multiple genes that are differentially expressed in regressor tumors (Figure S1), thus indicating that IL-17D is one of many genes that could participate in tumor surveillance. This is likely due to the heterogeneity and redundancy that is inherent in our system (and possibly in normal tumor surveillance mechanisms). For example, we have found that some regressors are well recognized by NK cells whereas others are not, and this is not always correlated with NKG2D ligand expression (O'Sullivan et al., 2011), even though NK cells and NKG2D are important for tumor surveillance (Guerra et al., 2008; Smyth et al., 2005). Furthermore, some regressors require type I interferon for their rejection whereas others do not (Dunn et al., 2005), even though $IFNAR^{-/-}$ mice lacking interferon α/β (IFNα/β) responsiveness are more susceptible to cancer (Diamond et al., 2011; Dunn et al., 2005; Fuertes et al., 2011), and IFNα/β is used in the treatment of melanoma (Garbe et al., 2011). We therefore conclude that IL-17D is one of many genes that regressor cells produce that can stimulate antitumor immunity. The identification of other genes that can differentiate regressor from progressor cell lines will involve future studies likely combining proteomic, gene expression, and exome sequencing approaches (Matsushita et al., 2012).

NK cells are known to be integral mediators of tumor surveillance (Bui and Schreiber, 2007; Smyth et al., 2001), but little is known about how they are recruited to sites of stress or transformation. Interestingly, in a model of liver carcinoma, the process of senescence induced MCP-1 and increased NK cell infiltration, leading to tumor suppression (Xue et al., 2007; Iannello et al., 2013), but IL-17D was not measured in this study. A recent study showed that the novel chemokine chemerin can recruit NK cells to mediate tumor surveillance (Pachynski et al., 2012), but it remains unclear what induces chemerin during inflammation. The chemokine receptor CXCR3 is expressed on NK cells (Uppaluri et al., 2008) and it ligands ITAC, MIG, and IP-10 can be induced by interferons during tumor development, but this receptor-ligand axis is not involved in the surveillance of MCA-induced sarcomas (Winkler et al., 2011). On the other hand, CXCR3 is thought to be the receptor that mediates the recruitment of cytokine-secreting $CD27^{high}$ NK cells into lymph nodes (Martín-Fontecha et al., 2004; Watt et al., 2008), and it may be possible that IL-17D can also induce CXCR3 ligands, either directly or indirectly via NK cell production of IFNγ.

Other studies of IL-17 family members in tumor progression have focused on IL-17A and Th-17 cells. These studies have shown both tumor-promoting and tumor-inhibiting roles for IL-17A/Th-17 cells. For instance, transfection of IL-17A can augment the progression of human tumor cell lines transplanted in nude mice by increasing neovascularization (Numasaki et al., 2003, 2005; Tartour et al., 1999), whereas in a mouse syngeneic system, IL-17A promotes tumor rejection by boosting T cell responses (Benchetrit et al., 2002; Hirahara et al., 2001). Th17 cells have also been associated with tumor rejection and good

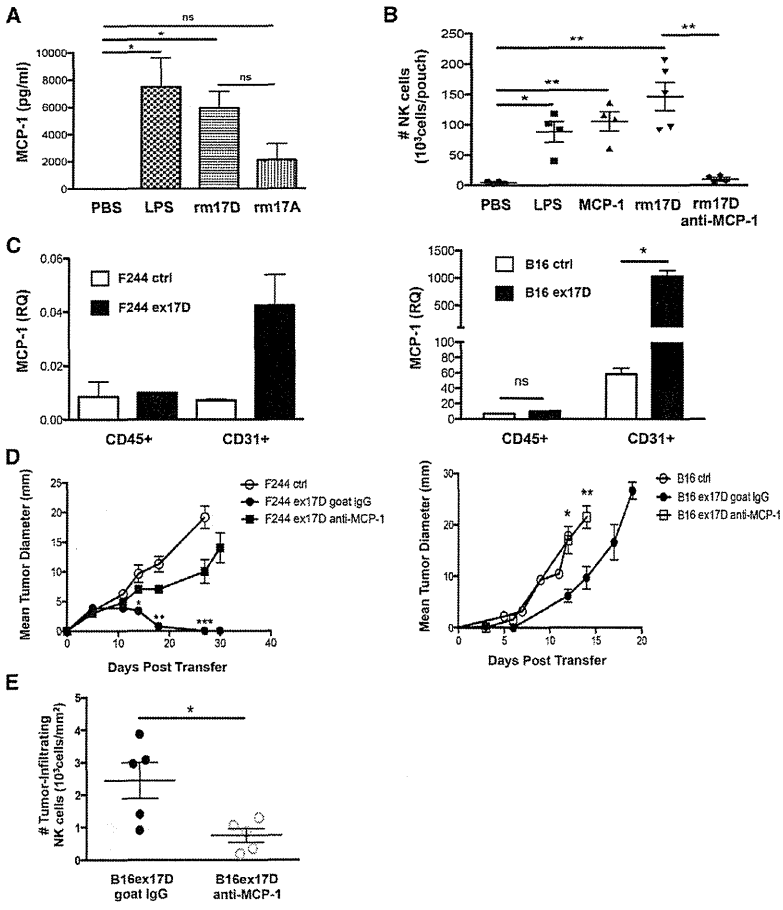

Figure 5. IL-17D Indirectly Recruits NK Cells through Tumor Endothelial Cell Production of MCP-1

(A) Air pouch lavage fluid chemokine levels of MCP-1.

(B) Total number of NK cells per air pouch for WT mice receiving intrapouch injections of PBS, LPS, IL-17A, IL-17D, MCP-1, or IL-17D and anti-MCP-1 monoclonal antibodies.

(C) qRT-PCR analysis of MCP-1 expression from purified tumor leukocytes and endothelial cells harvested from day 7 F244 or B16.OVA control or ex17D tumors.

(D) Tumor growth of F244 or B16 OVA control and ex17D tumors transplanted into WT mice receiving either intraperitoneal (i.p.) injections of goat polyclonal anti-MCP-1 or control goat IgG.

(E) Number of tumor-infiltrating NK cells per square mm of tumor from day 7 B16 OVA ex17D tumors transplanted into WT mice receiving either i.p. injections of goat polyclonal anti-MCP-1 or control goat IgG.

Data are representative of two independent experiments. Each point represents a single mouse. Samples were compared using an unpaired, two-tailed Student's t test with Welch's correction. Error bars are depicted as ±SEM (*$p < 0.05$, **$p < 0.01$, ***$p < 0.001$; NS, not significant). See also Figure S5.

prognosis in some studies (Kryczek et al., 2007; Muranski et al., 2008), whereas other studies indicate that Th17 cells promote tumor growth (Xiao et al., 2009; Zhang et al., 2008). One potential explanation for these conflicting results is that IL-17A can activate and recruit neutrophils, which recently have been shown to have both tumor-promoting and tumor-inhibiting activities (Fridlender et al., 2009). In contrast, it is well established that NK cells have antitumor activities (Bui and Schreiber, 2007; Smyth et al., 2001) and in fact can promote antitumor T cell (Diefenbach et al., 2001; Kelly et al., 2002) (Figure 2C) and macrophage responses (O'Sullivan et al., 2012) (Figure 3D). Therefore, unlike IL-17A, IL-17D may induce more consistent antitumor responses through NK cell recruitment that could be more effectively translated to cancer immune therapy. On the other hand, because enforced IL-17D expression induced rejection of some, but not all, progressor cell lines, it is likely that IL-17D-based therapy, acting through NK cells, will need to be used in combination with checkpoint blockade or inhibitors of T regulatory cells, which can prevent NK cell activation (Ghiringhelli et al., 2005; Smyth et al., 2006). It is not clear what the total effect enforced IL-17D expression would have on adaptive immunity, but nevertheless, adaptive immunity is required (Figure S2) and induced (Figure 3C) in IL-17D-mediated rejection. Finally, we speculate that the selective expression of IL-17D in neoplastic cells as opposed to immune cells would translate to a more benign side effect profile, because this ancient cytokine may have evolved to mediate early, and clinically silent, innate tissue surveillance of stress, transformation, and/or pathogen infection.

EXPERIMENTAL PROCEDURES

All experiments involving mice were conducted under animal protocols approved by the Washington University Animal Studies Committee and the University of California, San Diego Institutional Animal Care and Use Committee (IACUC protocol #S06201) and were in accordance with their ethical guidelines.

Cell Lines and Mice

MCA sarcoma cell lines are a kind gift from Dr. Robert Schreiber and were generated as described previously (Shankaran et al., 2001). All experiments were done with cells passaged between 4 and 12 cycles. 129/Sv, C57BL/6 × 129/Sv F1, 129/Sv RAG2$^{-/-}$, C57BL/6 RAG2$^{-/-}$, and RAG2$^{-/-}$ × $\gamma c^{-/-}$ mice used were used for tumor transplantation experiments. Cell lines were maintained in RPMI 1640 supplemented with 10% fetal calf serum, L-glutamine, nonessential amino acids, sodium pyruvate, sodium bicarbonate, penicillin/streptomycin, and β-mercaptoethanol.

Microarray and Clustering Analysis

Murine Genome U74v2 Set GeneChip Array (Affymetrix) was used for analysis of cDNA generated from regressor and progressor tumor cell lines. Details of RNA preparation, cDNA preparation, microarray setup, and clustering analysis are described in the Supplemental Experimental Procedures.

Human Cancer Microarray Data Analysis

For human clinical samples, *IL-17D* gene expression was evaluated from NCBI GEO data sets from studies comparing primary and metastatic tumors (GDS2546) or low-grade versus high-grade glioma patient samples (GDS4467, GDS1976, and GDS1816) as described previously (Pachynski et al., 2012).

Generation of IL-17D-Deficient and Overexpressing Tumor Cell Lines

Cell lines were generated as described in the Supplemental Experimental Procedures.

Antibodies and FACS Analysis of Tumor Cells

For intracellular staining, cells were either incubated with or without 2 μM monensin (Sigma) and 1 μg/ml Brefeldin A (BD Biosciences) and then harvested by trypsinization, washed once with PBS, stained, and analyzed for intracellular IL-17D signal as described in the Supplemental Experimental Procedures.

Tumor Transplantation and TIL Analysis

Subconfluent tumor cell lines were harvested and injected subcutaneously into syngeneic recipient WT, RAG2$^{-/-}$, or RAG2$^{-/-}$ × γc$^{-/-}$ mice at either 1 × 10^6 cells/mouse (for all growth experiments) or 5–10 × 10^6 cells/mouse (for tumor-infiltrating leukocyte [TIL] analysis), as previously described (Bui et al., 2006). Tumor rechallenge was performed 3 months after mice had rejected transplanted tumors by injecting 1 × 10^6 cells per mouse subcutaneously with parental tumor cell lines. In vivo depletion of various immune subsets, doxycycline administration, and intratumoral injection of IL-17D are described in the Supplemental Experimental Procedures. Tumor growth and immune infiltration were analyzed as described in the Supplemental Experimental Procedures.

Mouse Air Pouch Experiments

C57BL/6 × 129/Sv F1 mice were injected subcutaneously with 3 ml of sterilized air filtered through a 0.2 μm Millipore filter (Bellerica) to form air pouches on day 0 and reinflated again on day 3. On day 7, 1 ml of LPS (1 μg/ml), IL-17A (5 μg/ml) (R&D Systems), IL-17D (5 μg/ml) (R&D Systems), IL-17D (5 μg/ml) (Mayfield Lab), MCP-1 (5 μg/ml) (Peprotech), or IL-17D (5 μg/ml) + anti-MCP-1 polyclonal antibodies (25 μg/ml) (R&D Systems) was injected into mouse air pouches 8 hr before air pouch harvest. Air pouches were lavaged with 2 ml PBS and centrifuged at 1,250 rpm for 5 min at room temperature. Supernatant was harvested and analyzed for chemokine protein levels using the mouse Chemokine FlowCytomix kit from eBioscience. Infiltrating air pouch cells were resuspended in FACS stain buffer, counted on a hemocytometer, and analyzed by cell-surface markers as described in the Supplemental Experimental Procedures.

Chemokine Secretion Assay

On days 7 and 14 posttransplantation, tumors were harvested and single-cell suspensions were prepared as described for the TIL analysis. Filtered tumor/immune cell suspensions were plated in triplicate wells at 40,000 cells per well in 100 μl for 24 hr at 37°C. Supernatant was analyzed for chemokines using the mouse chemokine flowcytomix kit from eBioscience.

Generation of cDNA and Quantitative PCR

Tumor cell lines were plated in triplicate at 6 × 10^4 cells/well in a six-well plate and incubated for 48 hr at 37°C. Supernatant was aspirated and cells were washed twice with PBS before addition of 1 ml TRIzol reagent (Invitrogen). CD31$^+$ and CD45$^+$ tumor-derived cell populations were washed twice with PBS before addition of 1 ml TRIzol reagent (Invitrogen). Details describing RNA extraction, cDNA preparation, quantitative PCR reactions, and analysis are described in the Supplemental Experimental Procedures.

SUPPLEMENTAL INFORMATION

Supplemental Information includes Supplemental Experimental Procedures and five figures and can be found with this article online at http://dx.doi.org/10.1016/j.celrep.2014.03.073.

ACKNOWLEDGMENTS

We would like to thank C. Peinado for assistance with tumor mixing, P. Lee for cloning assistance, and R. Schreiber for critical review of the manuscript. J.D.B. is supported by grants from the Hartwell Foundation, NIH (CA128893 and CA157885), the American Cancer Society (ACS-IRG #70-002), the Cancer Research Coordinating Committee (6-444951-34384), and the Concern Foundation. Funds for IL-17D production in the S.P.M. lab came from the California Energy Commission award 500-10-039.

Received: August 21, 2012
Revised: January 8, 2014
Accepted: March 31, 2014
Published: May 1, 2014

REFERENCES

Benchetrit, F., Ciree, A., Vives, V., Warnier, G., Gey, A., Sautès-Fridman, C., Fossiez, F., Haicheur, N., Fridman, W.H., and Tartour, E. (2002). Interleukin-17 inhibits tumor cell growth by means of a T-cell-dependent mechanism. Blood *99*, 2114–2121.

Bierie, B., and Moses, H.L. (2010). Transforming growth factor beta (TGF-beta) and inflammation in cancer. Cytokine Growth Factor Rev. *21*, 49–59.

Bonmort, M., Dalod, M., Mignot, G., Ullrich, E., Chaput, N., and Zitvogel, L. (2008). Killer dendritic cells: IKDC and the others. Curr. Opin. Immunol. *20*, 558–565.

Boon, T., and van der Bruggen, P. (1996). Human tumor antigens recognized by T lymphocytes. J. Exp. Med. *183*, 725–729.

Bui, J.D., and Schreiber, R.D. (2007). Cancer immunosurveillance, immunoediting and inflammation: independent or interdependent processes? Curr. Opin. Immunol. *19*, 203–208.

Bui, J.D., Uppaluri, R., Hsieh, C.S., and Schreiber, R.D. (2006). Comparative analysis of regulatory and effector T cells in progressively growing versus rejecting tumors of similar origins. Cancer Res. *66*, 7301–7309.

Diamond, M.S., Kinder, M., Matsushita, H., Mashayekhi, M., Dunn, G.P., Archambault, J.M., Lee, H., Arthur, C.D., White, J.M., Kalinke, U., et al. (2011). Type I interferon is selectively required by dendritic cells for immune rejection of tumors. J. Exp. Med. *208*, 1989–2003.

Diefenbach, A., Jensen, E.R., Jamieson, A.M., and Raulet, D.H. (2001). Rae1 and H60 ligands of the NKG2D receptor stimulate tumour immunity. Nature *413*, 165–171.

Dranoff, G. (2004). Cytokines in cancer pathogenesis and cancer therapy. Nat. Rev. Cancer *4*, 11–22.

Dranoff, G., Jaffee, E., Lazenby, A., Golumbek, P., Levitsky, H., Brose, K., Jackson, V., Hamada, H., Pardoll, D., and Mulligan, R.C. (1993). Vaccination with irradiated tumor cells engineered to secrete murine granulocyte-macrophage colony-stimulating factor stimulates potent, specific, and long-lasting anti-tumor immunity. Proc. Natl. Acad. Sci. USA *90*, 3539–3543.

Dunn, G.P., Bruce, A.T., Sheehan, K.C., Shankaran, V., Uppaluri, R., Bui, J.D., Diamond, M.S., Koebel, C.M., Arthur, C., White, J.M., and Schreiber, R.D. (2005). A critical function for type I interferons in cancer immunoediting. Nat. Immunol. *6*, 722–729.

DuPage, M., Mazumdar, C., Schmidt, L.M., Cheung, A.F., and Jacks, T. (2012). Expression of tumour-specific antigens underlies cancer immunoediting. Nature *482*, 405–409.

Flood, P.M., Schreiber, H., and Ron, Y. (1987). Protective immunity to progressive tumors can be induced by antigen presented on regressor tumors. J. Immunol. *138*, 3573–3579.

Fridlender, Z.G., Sun, J., Kim, S., Kapoor, V., Cheng, G., Ling, L., Worthen, G.S., and Albelda, S.M. (2009). Polarization of tumor-associated neutrophil phenotype by TGF-beta: "N1" versus "N2" TAN. Cancer Cell *16*, 183–194.

Fuertes, M.B., Kacha, A.K., Kline, J., Woo, S.R., Kranz, D.M., Murphy, K.M., and Gajewski, T.F. (2011). Host type I IFN signals are required for antitumor

CD8+ T cell responses through CD8alpha+ dendritic cells. J. Exp. Med. *208*, 2005–2016.

Garbe, C., Eigentler, T.K., Keilholz, U., Hauschild, A., and Kirkwood, J.M. (2011). Systematic review of medical treatment in melanoma: current status and future prospects. Oncologist *16*, 5–24.

Ghiringhelli, F., Ménard, C., Terme, M., Flament, C., Taieb, J., Chaput, N., Puig, P.E., Novault, S., Escudier, B., Vivier, E., et al. (2005). CD4+CD25+ regulatory T cells inhibit natural killer cell functions in a transforming growth factor-beta-dependent manner. J. Exp. Med. *202*, 1075–1085.

Guerra, N., Tan, Y.X., Joncker, N.T., Choy, A., Gallardo, F., Xiong, N., Knoblaugh, S., Cado, D., Greenberg, N.M., and Raulet, D.H. (2008). NKG2D-deficient mice are defective in tumor surveillance in models of spontaneous malignancy. Immunity *28*, 571–580.

Hirahara, N., Nio, Y., Sasaki, S., Minari, Y., Takamura, M., Iguchi, C., Dong, M., Yamasawa, K., and Tamura, K. (2001). Inoculation of human interleukin-17 gene-transfected Meth-A fibrosarcoma cells induces T cell-dependent tumor-specific immunity in mice. Oncology *61*, 79–89.

Hutson, T.E. (2011). Targeted therapies for the treatment of metastatic renal cell carcinoma: clinical evidence. Oncologist *16* (*Suppl 2*), 14–22.

Iannello, A., Thompson, T.W., Ardolino, M., Lowe, S.W., and Raulet, D.H. (2013). p53-dependent chemokine production by senescent tumor cells supports NKG2D-dependent tumor elimination by natural killer cells. J. Exp. Med. *210*, 2057–2069.

Iwakura, Y., Ishigame, H., Saijo, S., and Nakae, S. (2011). Functional specialization of interleukin-17 family members. Immunity *34*, 149–162.

Johansen, C., Usher, P.A., Kjellerup, R.B., Lundsgaard, D., Iversen, L., and Kragballe, K. (2009). Characterization of the interleukin-17 isoforms and receptors in lesional psoriatic skin. Br. J. Dermatol. *160*, 319–324.

Kelly, J.M., Darcy, P.K., Markby, J.L., Godfrey, D.I., Takeda, K., Yagita, H., and Smyth, M.J. (2002). Induction of tumor-specific T cell memory by NK cell-mediated tumor rejection. Nat. Immunol. *3*, 83–90.

Kolls, J.K., and Lindén, A. (2004). Interleukin-17 family members and inflammation. Immunity *21*, 467–476.

Kryczek, I., Wei, S., Zou, L., Altuwaijri, S., Szeliga, W., Kolls, J., Chang, A., and Zou, W. (2007). Cutting edge: Th17 and regulatory T cell dynamics and the regulation by IL-2 in the tumor microenvironment. J. Immunol. *178*, 6730–6733.

Liu, R.B., Engels, B., Arina, A., Schreiber, K., Hyjek, E., Schietinger, A., Binder, D.C., Butz, E., Krausz, T., Rowley, D.A., et al. (2012). Densely granulated murine NK cells eradicate large solid tumors. Cancer Res. *72*, 1964–1974.

Martín-Fontecha, A., Thomsen, L.L., Brett, S., Gerard, C., Lipp, M., Lanzavecchia, A., and Sallusto, F. (2004). Induced recruitment of NK cells to lymph nodes provides IFN-gamma for T(H)1 priming. Nat. Immunol. *5*, 1260–1265.

Matsushita, H., Vesely, M.D., Koboldt, D.C., Rickert, C.G., Uppaluri, R., Magrini, V.J., Arthur, C.D., White, J.M., Chen, Y.S., Shea, L.K., et al. (2012). Cancer exome analysis reveals a T-cell-dependent mechanism of cancer immunoediting. Nature *482*, 400–404.

Müller, A., and Lamprecht, P. (2008). [Interleukin-17 in chronic inflammatory and autoimmune diseases: rheumatoid arthritis, Crohn's disease and Wegener's granulomatosis]. Z. Rheumatol. *67*, 72–74.

Muranski, P., Boni, A., Antony, P.A., Cassard, L., Irvine, K.R., Kaiser, A., Paulos, C.M., Palmer, D.C., Touloukian, C.E., Ptak, K., et al. (2008). Tumor-specific Th17-polarized cells eradicate large established melanoma. Blood *112*, 362–373.

Nicholas, C., and Lesinski, G.B. (2011). Immunomodulatory cytokines as therapeutic agents for melanoma. Immunotherapy *3*, 673–690.

Numasaki, M., Fukushi, J., Ono, M., Narula, S.K., Zavodny, P.J., Kudo, T., Robbins, P.D., Tahara, H., and Lotze, M.T. (2003). Interleukin-17 promotes angiogenesis and tumor growth. Blood *101*, 2620–2627.

Numasaki, M., Watanabe, M., Suzuki, T., Takahashi, H., Nakamura, A., McAllister, F., Hishinuma, T., Goto, J., Lotze, M.T., Kolls, J.K., and Sasaki, H. (2005). IL-17 enhances the net angiogenic activity and in vivo growth of human non-small cell lung cancer in SCID mice through promoting CXCR-2-dependent angiogenesis. J. Immunol. *175*, 6177–6189.

O'Sullivan, T., Dunn, G.P., Lacoursiere, D.Y., Schreiber, R.D., and Bui, J.D. (2011). Cancer immunoediting of the NK group 2D ligand H60a. J. Immunol. *187*, 3538–3545.

O'Sullivan, T., Saddawi-Konefka, R., Vermi, W., Koebel, C.M., Arthur, C., White, J.M., Uppaluri, R., Andrews, D.M., Ngiow, S.F., Teng, M.W., et al. (2012). Cancer immunoediting by the innate immune system in the absence of adaptive immunity. J. Exp. Med. *209*, 1869–1882.

Pachynski, R.K., Zabel, B.A., Kohrt, H.E., Tejeda, N.M., Monnier, J., Swanson, C.D., Holzer, A.K., Gentles, A.J., Sperinde, G.V., Edalati, A., et al. (2012). The chemoattractant chemerin suppresses melanoma by recruiting natural killer cell antitumor defenses. J. Exp. Med. *209*, 1427–1435.

Pappu, R., Ramirez-Carrozzi, V., and Sambandam, A. (2011). The interleukin-17 cytokine family: critical players in host defence and inflammatory diseases. Immunology *134*, 8–16.

Paul, W. (2013). Fundamental Immunology, Seventh Edition (Philadelphia: Lippincott Williams & Wilkins).

Pelletier, M., Bouchard, A., and Girard, D. (2004). In vivo and in vitro roles of IL-21 in inflammation. J. Immunol. *173*, 7521–7530.

Ramirez-Carrozzi, V., Sambandam, A., Luis, E., Lin, Z., Jeet, S., Lesch, J., Hackney, J., Kim, J., Zhou, M., Lai, J., et al. (2011). IL-17C regulates the innate immune function of epithelial cells in an autocrine manner. Nat. Immunol. *12*, 1159–1166.

Roberts, S., Gueguen, Y., de Lorgeril, J., and Goetz, F. (2008). Rapid accumulation of an interleukin 17 homolog transcript in Crassostrea gigas hemocytes following bacterial exposure. Dev. Comp. Immunol. *32*, 1099–1104.

Rosenblatt, J., and McDermott, D.F. (2011). Immunotherapy for renal cell carcinoma. Hematol. Oncol. Clin. North Am. *25*, 793–812.

Roussel, L., Houle, F., Chan, C., Yao, Y., Bérubé, J., Olivenstein, R., Martin, J.G., Huot, J., Hamid, Q., Ferri, L., and Rousseau, S. (2010). IL-17 promotes p38 MAPK-dependent endothelial activation enhancing neutrophil recruitment to sites of inflammation. J. Immunol. *184*, 4531–4537.

Schreiber, R.D., Old, L.J., and Smyth, M.J. (2011). Cancer immunoediting: integrating immunity's roles in cancer suppression and promotion. Science *331*, 1565–1570.

Shankaran, V., Ikeda, H., Bruce, A.T., White, J.M., Swanson, P.E., Old, L.J., and Schreiber, R.D. (2001). IFNgamma and lymphocytes prevent primary tumour development and shape tumour immunogenicity. Nature *410*, 1107–1111.

Smyth, M.J., Godfrey, D.I., and Trapani, J.A. (2001). A fresh look at tumor immunosurveillance and immunotherapy. Nat. Immunol. *2*, 293–299.

Smyth, M.J., Swann, J., Cretney, E., Zerafa, N., Yokoyama, W.M., and Hayakawa, Y. (2005). NKG2D function protects the host from tumor initiation. J. Exp. Med. *202*, 583–588.

Smyth, M.J., Teng, M.W., Swann, J., Kyparissoudis, K., Godfrey, D.I., and Hayakawa, Y. (2006). CD4+CD25+ T regulatory cells suppress NK cell-mediated immunotherapy of cancer. J. Immunol. *176*, 1582–1587.

Song, X., Zhu, S., Shi, P., Liu, Y., Shi, Y., Levin, S.D., and Qian, Y. (2011). IL-17RE is the functional receptor for IL-17C and mediates mucosal immunity to infection with intestinal pathogens. Nat. Immunol. *12*, 1151–1158.

Starnes, T., Broxmeyer, H.E., Robertson, M.J., and Hromas, R. (2002). Cutting edge: IL-17D, a novel member of the IL-17 family, stimulates cytokine production and inhibits hemopoiesis. J. Immunol. *169*, 642–646.

Tartour, E., Fossiez, F., Joyeux, I., Galinha, A., Gey, A., Claret, E., Sastre-Garau, X., Couturier, J., Mosseri, V., Vives, V., et al. (1999). Interleukin 17, a T-cell-derived cytokine, promotes tumorigenicity of human cervical tumors in nude mice. Cancer Res. *59*, 3698–3704.

Terme, M., Ullrich, E., Aymeric, L., Meinhardt, K., Coudert, J.D., Desbois, M., Ghiringhelli, F., Viaud, S., Ryffel, B., Yagita, H., et al. (2012). Cancer-induced

immunosuppression: IL-18-elicited immunoablative NK cells. Cancer Res. *72*, 2757–2767.

Uppaluri, R., Sheehan, K.C., Wang, L., Bui, J.D., Brotman, J.J., Lu, B., Gerard, C., Hancock, W.W., and Schreiber, R.D. (2008). Prolongation of cardiac and islet allograft survival by a blocking hamster anti-mouse CXCR3 monoclonal antibody. Transplantation *86*, 137–147.

Vaage, J. (1971). Concomitant immunity and specific depression of immunity by residual or reinjected syngeneic tumor tissue. Cancer Res. *31*, 1655–1662.

Watt, S.V., Andrews, D.M., Takeda, K., Smyth, M.J., and Hayakawa, Y. (2008). IFN-gamma-dependent recruitment of mature CD27(high) NK cells to lymph nodes primed by dendritic cells. J. Immunol. *181*, 5323–5330.

Winkler, A.E., Brotman, J.J., Pittman, M.E., Judd, N.P., Lewis, J.S., Jr., Schreiber, R.D., and Uppaluri, R. (2011). CXCR3 enhances a T-cell-dependent epidermal proliferative response and promotes skin tumorigenesis. Cancer Res. *71*, 5707–5716.

Xiao, M., Wang, C., Zhang, J., Li, Z., Zhao, X., and Qin, Z. (2009). IFNgamma promotes papilloma development by up-regulating Th17-associated inflammation. Cancer Res. *69*, 2010–2017.

Xue, W., Zender, L., Miething, C., Dickins, R.A., Hernando, E., Krizhanovsky, V., Cordon-Cardo, C., and Lowe, S.W. (2007). Senescence and tumour clearance is triggered by p53 restoration in murine liver carcinomas. Nature *445*, 656–660.

Zhang, B., Rong, G., Wei, H., Zhang, M., Bi, J., Ma, L., Xue, X., Wei, G., Liu, X., and Fang, G. (2008). The prevalence of Th17 cells in patients with gastric cancer. Biochem. Biophys. Res. Commun. *374*, 533–537.

Zitvogel, L., Tesniere, A., and Kroemer, G. (2006). Cancer despite immunosurveillance: immunoselection and immunosubversion. Nat. Rev. Immunol. *6*, 715–727.

Zou, W., and Chen, L. (2008). Inhibitory B7-family molecules in the tumour microenvironment. Nat. Rev. Immunol. *8*, 467–477.

European Journal of Immunology

Stimulation through very late antigen-4 and -5 improves the multifunctionality and memory formation of CD8$^+$ T cells

Hayato Hosoi[1,2], Hiroaki Ikeda[1], Naoko Imai[1], Chisaki Amaike[1], Linan Wang[1], Yuki Orito[1], Makiko Yamane[1], Hiroaki Ueno[1], Mitsuko Ideno[3], Ikuei Nukaya[3], Tatsuji Enoki[3], Junichi Mineno[3], Kazutoh Takesako[3], Satoshi Hirano[2] and Hiroshi Shiku[1]

[1] Department of Immuno-Gene Therapy, Mie University Graduate School of Medicine, Tsu, Japan
[2] Department of Surgical Oncology, Hokkaido University Graduate School of Medicine, Sapporo, Japan
[3] Center for Cell and Gene Therapy, Takara Bio Inc., Otsu, Japan

T cells express multiple integrin molecules. The significance of signaling through these molecules on acquisition of T-cell effector functions and memory formation capacity remains largely unknown. Moreover, the impact of stimulation through these signals on the generation of T cells for adoptive immunotherapy has not been elucidated. In this study, using a recombinant fragment of fibronectin, CH-296, we demonstrated that stimulation via very late Ag (VLA)-4 and VLA-5 in human and BALB/c mouse CD8$^+$ T cells, in combination with TCR stimulation, enhances effector multifunctionality and in vivo memory formation. Using TCR-transgenic mouse-derived CD8$^+$ T cells expressing TCR specific for the syngeneic CMS5 fibrosarcoma-derived tumor Ag, we showed that stimulation by CH-296 improved the ability of tumor-specific CD8$^+$ T cells to inhibit CMS5 tumor growth when adoptively transferred into hosts with progressing tumors. Improved antitumor effects were associated with decreased infiltration of Foxp3$^+$CD4$^+$ Treg cells in tumors. These results suggest that stimulation via VLA-4 and VLA-5 modulates the qualities of effector T cells and could potentially increase the efficacy of adoptive therapy against cancer.

Keywords: CD8$^+$ T cells · Integrins · Multifunctionality · Tumor immunology · Very late antigen (VLA)

Additional supporting information may be found in the online version of this article at the publisher's web-site

Introduction

T cells express a number of surface molecules that mediate cell-to-cell interactions, as well as binding of cells to extracellular matrix proteins [1–3]. Several of these adhesion receptors belong to the β1 subfamily of integrin molecules, also known as very late Ag (VLA) molecules, which are characterized by at least nine α-chains

Correspondence: Dr. Hiroaki Ikeda
e-mail: hikeda@clin.medic.mie-u.ac.jp

that share a noncovalently linked β-chain. Some of these receptors function not only as adhesion molecules but also as transducers of signals in T cells [3–6]. Several laboratories have shown that binding of human or mouse T cells to fibronectin can induce proliferation via VLA-4 (α4β1) and/or VLA-5 (α5β1) [7–9]. Consistent with these reports, we have shown that exposure to CH-296 (RetroNectin), a recombinant human fibronectin fragment that contains the binding domains for VLA-4 and -5, in conjunction with stimulation with anti-CD3 mAbs, promotes T-cell expansion while preserving the $CD45RA^{high}CCR7^{high}$ phenotype [10]. These results prompted us to investigate whether stimulation via VLA-4 and -5 modulates not only expansion of T cells but also their effector functions and in vivo fates.

Cytotoxic T lymphocytes (CTLs) play critical roles in controlling tumor cells [11, 12], and the adoptive cell transfer of tumor-reactive CTLs is a promising strategy for immunological intervention against cancer [12–14]. For clinical applications, T cells of desired specificities have been isolated from patients or genetically engineered to express specific receptors that target tumor cells, followed by expansion in culture prior to transfer [12–14]. This strategy is intended to overcome both the low frequency of precursors of high-avidity tumor-reacting T cells in patients and the difficulty of inducing in vivo expansion of these cells in the immunosuppressive microenvironments associated with tumor-bearing hosts [12–14]. However, the efficacy of adoptive T-cell therapy has been limited in both humans and animal models, in part due to the failure of cultured T cells to persist and function properly following transfer [15, 16].

The primary objective of this study was to explore the biological impact of signals through VLA-4/5 on the functional qualities of $CD8^+$ T cells. We evaluated the multifunctionality (polyfunctionality) of human and mouse T cells expanded by stimulation with CH-296 and anti-CD3, and tested the in vivo memory formation ability of the murine T cells. In addition, we tested the influence of stimulation via VLA-4/5 on the antitumor effect of tumor-specific T cells in adoptive immunotherapy using tumor Ag-specific TCR-transgenic mouse-derived T cells.

Results

CH-296 stimuli on TCR engagement enhances multifunctionality in $CD8^+$ T cells upon recall response

We reported previously that simultaneous stimulation of human PBMCs with a CH-296 and anti-CD3 mAb significantly increased their expansion relative to stimulation with anti-CD3 alone [10]. We have confirmed that the interaction with CH-296 upon TCR engagement promotes the expansion of $CD8^+$ T cells, both by increasing their proliferation and by inhibiting apoptosis (data not shown). However, the impact of fibronectin-mediated stimulation of T cells on their effector functions remains largely unknown. To address this issue, we cultured human T cells in plates coated with anti-CD3 mAb in the absence or presence of CH-296, and then re-stimulated these cells after 7 days in culture, in order to evaluate the recall expression of their effector functions. As shown in Figure 1A, the presence of CH-296 during the initial stimulation increased the secretion of IFN-γ and TNF-α during the recall response. The mobilization of CD107a, a marker for the release of cytotoxic granules, was also elevated in cells stimulated with CH-296. We previously reported that the multifunctionality of effector CTLs, as assessed by the combination of these three measurements, is a critical determinant of the quality of the T-cell response [17–19]. The acquisition of multifunctionality by effector T cells is one mechanism by which these cells resist immunosuppression mediated by tumor progression in a model of adoptive transfer of tumor-specific T cells [17–19]. We therefore evaluated multifunctionality by calculating the relative frequency of several distinct populations: cells with all three functional characteristics, cells with varying combinations of two functions, cells displaying only one function, and cells without any of these functions. The presence of CH-296 during the initial stimulation increased the multifunctionality of human $CD8^+$ T cells during the recall response (Fig. 1B).

Using in vitro-cultured TCR-transgenic mouse-derived T cells expressing an $H\text{-}2K^d$-restricted transgenic TCR specific for the syngeneic CMS5 fibrosarcoma-derived mutated ERK2 Ag, we evaluated the Ag-specific recall response of these cells. After initial stimulation of the TCR-transgenic mouse-derived T cells by anti-CD3 mAb, with or without CH-296, we re-stimulated these cells with Ag peptide and monitored production of IFN-γ and TNF-α and mobilization of CD107a. Similar to the case of human $CD8^+$ T cells, interaction with CH-296 during the initial stimulation significantly increased the expression of these effector functions in mouse $CD8^+$ T cells (Fig. 1C), in an Ag-specific manner, under our experimental conditions. Importantly, the proportion of multifunctional cells increased in T cells stimulated in the presence of CH-296 (Fig. 1D). Tri-functional and bi-functional cells were 30 and 35%, respectively, of cells stimulated with anti-CD3 plus CH-296. By contrast, cells with three and two functions were 5 and 20% of cells initially stimulated with anti-CD3 alone. No recall response against an irrelevant control peptide was observed (data not shown).

Stimulation through the co-stimulatory molecule CD28 is one of the most frequently used methods for enhancing the stimulatory properties of anti-CD3 mAb. Although anti-CD28 mAb increased the production of IFN-γ and TNF-α in T cells, CH-296 induced significantly higher populations of cells producing both of these cytokines during the recall response (Supporting Information Fig. 1A). Furthermore, stimulation by anti-CD3 plus CH-296 induced increased multifunctionality in $CD8^+$ T cells during recall response (Supporting Information Fig. 1B). In contrast, multifunctionality was higher in T cells stimulated with CD3/CD28 than in those stimulated with CD3/CH-296 at time points soon after the initial stimulation (Supporting Information Fig. 2). Moreover, CD3/CD28 stimulation of murine T cells induced more rapid proliferation than CD3/CH-296 stimulation (Supporting Information Fig. 3). These results suggested that the CD28 and CH-296 signals exerted different effects on T-cell quality and differentiation.

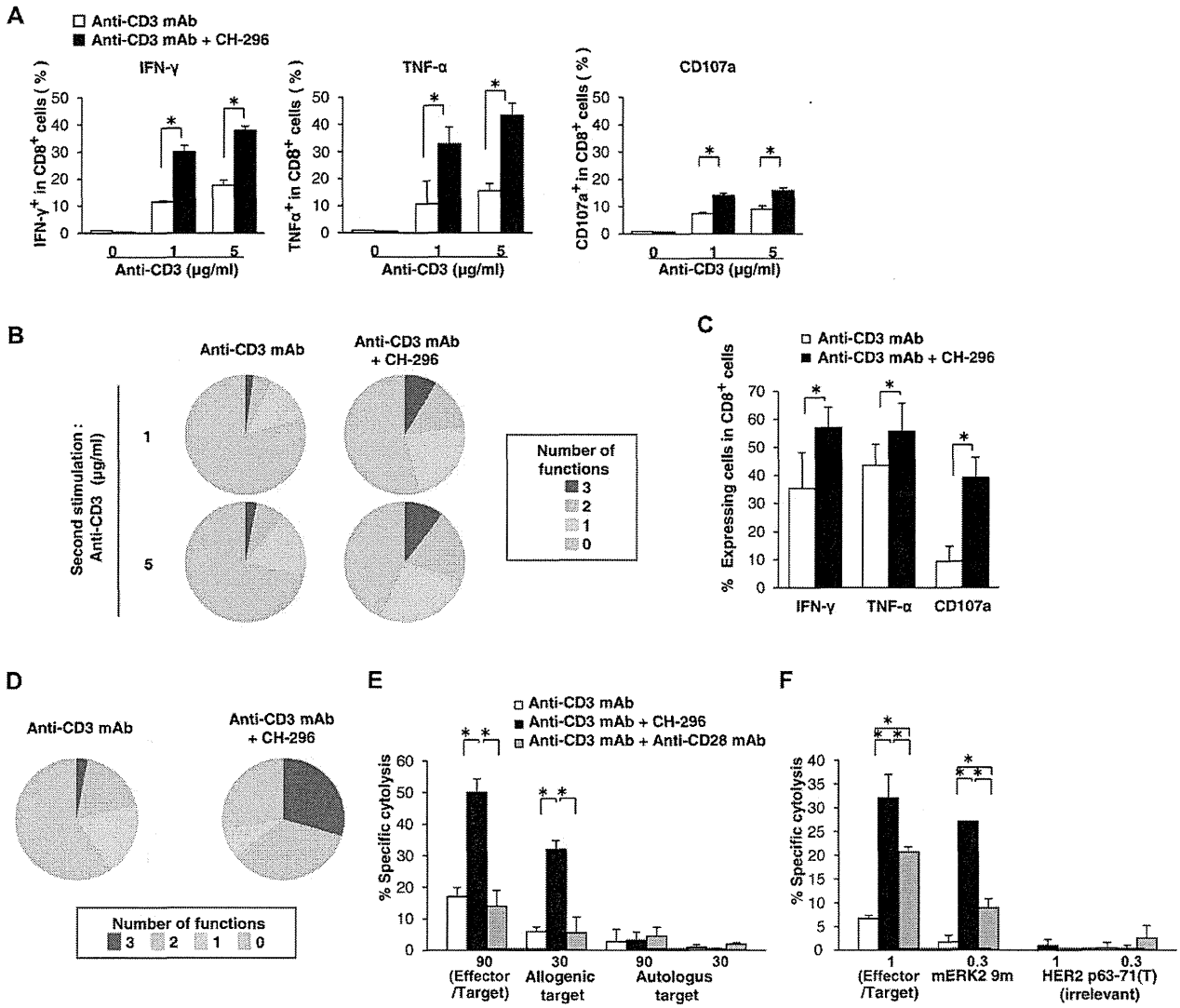

Figure 1. Multifunctionality in human and mouse CD8+ T cells during the recall response is promoted by CH-296 upon CD3 engagement. Human PBMCs (A, B, and E) or DUC18-Tg mouse-derived spleen cells (C, D, and F) were stimulated with or without CH-296 in combination with anti-CD3 mAb. (A) Seven days after stimulation, human PBMCs were re-stimulated with the indicated concentrations of anti-CD3 mAb coated on plates and then assayed for production of functional markers of CD8+ T cells (IFN-γ, TNF-α, and CD107a) by flow cytometry. Initial gating of each sample set utilized a forward scatter height (FSC-H) versus width (FSC-W) plot to remove doublets. Cells were then gated using forward scatter height (FSC-H) and side scatter area (SSC-A) to isolate small lymphocytes, followed by the gating to CD8+ cells. (B) Multifunctionality data from three independent PBMCs samples are summarized in the pie chart, in which each wedge represents the frequency of CD8+ T cells expressing all three functions (IFN-γ+TNF-α+CD107a+) (3), any two functions (IFN-γ+TNF-α+CD107a−, IFN-γ+TNF-α−CD107a+, or IFN-γ−TNF-α+CD107a+) (2), any single function (IFN-γ+TNF-α−CD107a−, IFN-γ−TNF-α+CD107a−, or IFN-γ−TNF-α−CD107a+) (1), or no function (0). (C) After 6 days of in vitro culture, DUC18-Tg mouse-derived spleen cells were re-stimulated with P1.HTR cells pulsed with 9m peptide, and then assayed for the frequency of CD8+ T cells exhibiting cytokine production and CD107a mobilization by flow cytometry. Initial gating of each sample set utilized FSC-H versus FSC-W plot to remove doublets. Cells were then gated using FSC-H and SSC-A to isolate small lymphocytes, followed by the gating to CD8+ cells. (D) Responses of three independent spleen cell samples are grouped and color-coded according to the number of acquired functions to determine multifunctionality. (E) After 7 days of stimulation with anti-CD3 in combination with CH-296, anti-CD28, or control solvent, human lymphocytes were mixed with allogeneic or autologous PHA-blast target cells at effector/target ratios of 90 and 30. Cytotoxicity was assessed by a calcein-AM release assay. (F) After 6 days of in vitro culture of DUC18-derived T cells with anti-CD3 in combination with CH-296, anti-CD28, or control solvent, cells were mixed with target P1.HTR cells pulsed with 9m or irrelevant peptide at effector/target ratios of 1 and 0.3. Cytotoxicity was assessed by a Cr-release assay. Data in A, C, E, and F represent the means + SD of three samples. (A–D) Results are representative of three independent experiments. (E, F) Results are representative of two independent experiments. Differences between groups were examined for statistical significance using Student's t-test. *$p < 0.05$.

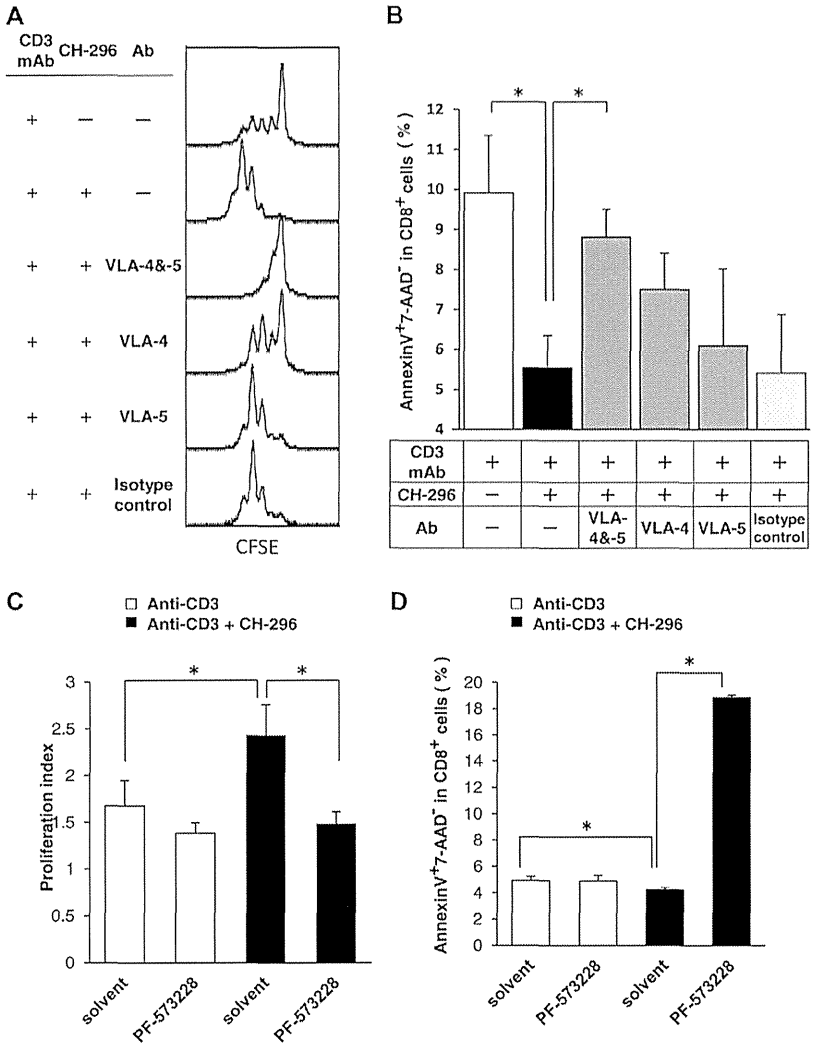

Figure 2. Activity of CH-296 in $CD8^+$ T cells is dependent on VLA-4, -5, and FAK. Mouse spleen cells were stimulated with anti-CD3/CH-296 either (A, B) in the presence or absence of neutralizing Abs against VLA-4 and -5 or isotype control (10 μg/mL each), or (C, D) in the presence or absence of FAK inhibitor (PF-573228, 2.5 μM) in triplicate cultures for 3 days. (A) Proliferation was assessed by flow-cytometry examining CFSE dilution in $CD8^+$-gated cells. (B) Frequency of Annexin $V^+7\text{-}AAD^-$ cells was assessed among $CD8^+$-gated cells by flow cytometry in the presence or absence of VLA-4/-5-specific Abs. (C) Proliferation index of CFSE-labeled $CD8^+$-gated cells in flow-cytometry analyses, as an average of the number of dividing cells, was calculated using the FlowJo software. (D) Frequency of Annexin $V^+7\text{-}AAD^-$ cells among $CD8^+$ cells was assessed by flow-cytometry analyses of $CD8^+$-gated cells in the presence of FAK inhibitor or control solvent. (B–D) Data are shown as means + SD of three samples and (A–D) are representative of three independent experiments. Differences between groups were examined for statistical significance using Student's t-test. $^*p < 0.05$.

CH-296 enhances Ag-specific cytotoxicity in $CD8^+$ T cells

Because CH-296 induced high expression of CD107a, we directly evaluated the Ag-specific cytotoxicity of $CD8^+$ T cells that had been stimulated in the presence or absence of CH-296. As shown in Figure 1E, human T cells stimulated with anti-CD3 mAb plus CH-296 exhibited higher cytotoxicity against allogeneic PHA-blast target cells than T cells stimulated with anti-CD3 mAb alone or anti-CD3 and anti-CD28 mAbs. T cells stimulated with anti-CD3 plus CH-296 did not lyse autologous target cells. $CD8^+$ T cells derived from TCR-transgenic mice stimulated in the presence of CH-296 also exhibited higher cytotoxicity against P1.HTR target cells pulsed with mutated ERK2-derived Ag peptide (mERK2 9m) than when they were stimulated in the absence of CH-296 (Fig. 1F). These cells did not lyse target cells pulsed with irrelevant $H\text{-}2K^d$-binding peptide.

CH-296 transduces a signal in mouse $CD8^+$ T cells through VLA-4, -5, and focal adhesion kinase

CH-296 contains CS1 and C domains that bind VLA-4 and -5, respectively. Using specific blocking Abs, we investigated whether stimulation of $CD8^+$ T cells by CH-296 is mediated by VLA-4 and -5. As shown in Figure 2A, blocking mAb against VLA-4 significantly inhibited the effect of CH-296 on the proliferation of $CD8^+$ T cells, as assessed by division of CFSE-labeled cells. The effect of anti-VLA-5 mAb alone was minimal, but the combination of anti-VLA-4 and -5 mAbs resulted in stronger inhibition of $CD8^+$ T-cell proliferation than when anti-VLA-4 was administered alone. Furthermore, CH-296 not only promoted proliferation but also inhibited induction of apoptosis in $CD8^+$ T cells. The combination of blocking mAbs against VLA-4 and -5 abrogated the inhibitory effect of CH-296 on apoptosis, as determined by induction of Annexin $V^+7\text{-}AAD^-$ cells (Fig. 2B).

The β1 integrin-mediated signals through the interaction with VLA-4 and -5, in combination with TCR signals, induce tyrosine phosphorylation of focal adhesion kinase ($pp125^{FAK}$; hereafter, FAK) [6]. We evaluated the effect of a FAK-specific inhibitor on CH-296-mediated proliferation and inhibition of apoptosis in mouse $CD8^+$ T cells. As shown in Figure 2C, FAK inhibitor abrogated the acceleration of $CD8^+$ T-cell proliferation by CH-296, as assessed by CFSE dilution. FAK inhibitor also induced increased apoptosis in $CD8^+$ T cells stimulated by CH-296 (Fig. 2D); these $CD8^+$ T cells became more apoptotic than cells stimulated with anti-CD3 alone. This observation suggests that stimulation through CH-296 may induce several signaling pathways in $CD8^+$ T cells that accelerate apoptosis when the FAK-mediated signal is absent.

Prolonged in vivo persistence of infused T cells stimulated with CH-296

We next addressed the in vivo persistence of adoptively transferred transgenic T cells in mice. TCR-Tg T cells stimulated in vitro with anti-CD3/CH-296 for 6 days exhibited a smaller proportion of cells with the $CD44^{high}CD62L^{low}$ terminally differentiated phenotype than cells stimulated with anti-CD3 alone or anti-CD3 and anti-CD28, as shown in Figure 3A and B. By contrast, anti-CD3/anti-CD28 stimulation resulted in fewer cells with the $CD44^{high}CD62L^{high}$ central/effector memory phenotype than other stimulation conditions. In addition, anti-CD3/CH-296 stimulation resulted in much less Tim3 expression than other conditions.

We adoptively transferred these T cells into mice. Forty-five days after the cell transfer, spleen cells were stained using the tetramer specific to the transgenic TCR. As shown in Figure 3C, $CD8^+$tetramer$^+$ T cells in mice that received T cells stimulated with anti-CD3 mAb plus CH-296 exhibited the $CD44^+CD62L^+CD127(IL\text{-}7R\alpha)^{high}$ memory T-cell phenotype. $CD8^+$tetramer$^+$ T cells in other groups exhibited a similar phenotype (data not shown). Thus, the persistence of infused T cells at day 45 indicates that these cells have the ability to form memory T-cell pools. When we calculated the total number of $CD8^+$tetramer$^+$ T cells in spleen, we observed higher persistence of tetramer-positive cells in mice that received transgenic T cells stimulated with anti-CD3 plus CH-296 than in mice that received T cells stimulated with anti-CD3 plus anti-CD28, anti-CD3 alone, or CH-296 alone (Fig. 3D).

We also investigated the long-term persistence of in vivo transferred T cells from a functional perspective. Specifically, we investigated the secondary response of the in vivo transferred T cells at the memory phase by measuring intracellular IFN-γ staining of spleen cells recalled with mutant ERK2 peptide- or control peptide-pulsed P1.HTR cells. As shown in Figure 3E, spleen cells in mice that received anti-CD3/CH-296-stimulated T cells exhibited a higher frequency of cells producing IFN-γ in an Ag-specific manner than cells in the other groups of mice.

Tumor-specific $CD8^+$ T cells primed with anti-CD3 and CH-296 efficiently inhibit tumor growth

Adoptive transfer of DUC18 TCR-transgenic mouse-derived $CD8^+$ T cells prevents subsequent CMS5 challenge [20]. However, we previously reported that CMS5 tumor progression inhibited the quality of transferred T cells, in part via induction of Treg cells, resulting in unsuccessful tumor control in a therapeutic context [17]. We found that depletion of Treg cells prior to tumor challenge increased the functionality of transferred tumor-specific T cells and retarded tumor growth, even when the T cells were transferred on day 7 of the tumor challenge [17]. We also observed that lymphodepleting pretreatments such as total body irradiation or administration of cyclophosphamide prior to adoptive T-cell transfer [16, 21, 22] increased the efficacy of adoptive cell therapy in hosts with progressing tumors (data not shown). In this study, we asked whether priming of tumor-specific $CD8^+$ T cells with a combination of anti-CD3 and CH-296 endowed T cells with the ability to inhibit tumor growth in hosts with progressing tumors, even without lymphodepleting pretreatment (Fig. 4). When adoptive T-cell transfer was performed on day 7 of tumor challenge, inhibition of tumor growth by DUC18-derived T cells stimulated with anti-CD3 alone was marginal (i.e. not statistically significantly different from the untreated control group). By contrast, tumor growth in mice receiving transgenic mouse-derived T cells primed with anti-CD3 in combination with CH-296 was significantly inhibited compared with the other groups. Transgenic mouse-derived T cells primed with anti-CD3 and anti-CD28 also efficiently inhibited CMS5 tumor growth; this effect was not statistically significantly different from that observed in the group stimulated with anti-CD3 and CH-296. Adoptive transfer of WT mouse-derived nonspecific T cells primed with anti-CD3 and CH-296, or DUC18-derived T cells primed by CH-296 alone, did not yield any antitumor effect.

Treg cells in tumor decreased in mice receiving tumor-specific $CD8^+$ T cells primed with CH-296

To investigate the immunosuppressive environment in tumor tissue of mice receiving adoptive cell therapy, we evaluated the frequency of $Foxp3^+$ $CD4^+$ Treg cells among $CD4^+$ T cells in CMS5 tumor tissue in mice receiving DUC18 mouse-derived T cells. As shown in Figure 5A and B, $Foxp3^+$ cells were less frequent in mice receiving T cells stimulated with anti-CD3 plus CH-296 than in mice treated with T cells stimulated with anti-CD3 alone. The CD8/CD4 ratio in tumor-infiltrating lymphocytes was elevated when T cells were stimulated with CH-296 (Fig. 5C). As a result, the CD8/Treg cells ratio was higher in mice receiving these T cells than in mice receiving T cells stimulated with anti-CD3 alone (Fig. 5D).

Next, we evaluated the relative levels of tumor infiltration of TCR-transgenic T cells by adoptively transferring CD90.1/DUC18 T cells into CD90.2 BALB/c mice. As shown in Figure 5E, the frequency of $CD90.1^+CD8^+$ T cells in tumor-infiltrating lymphocytes

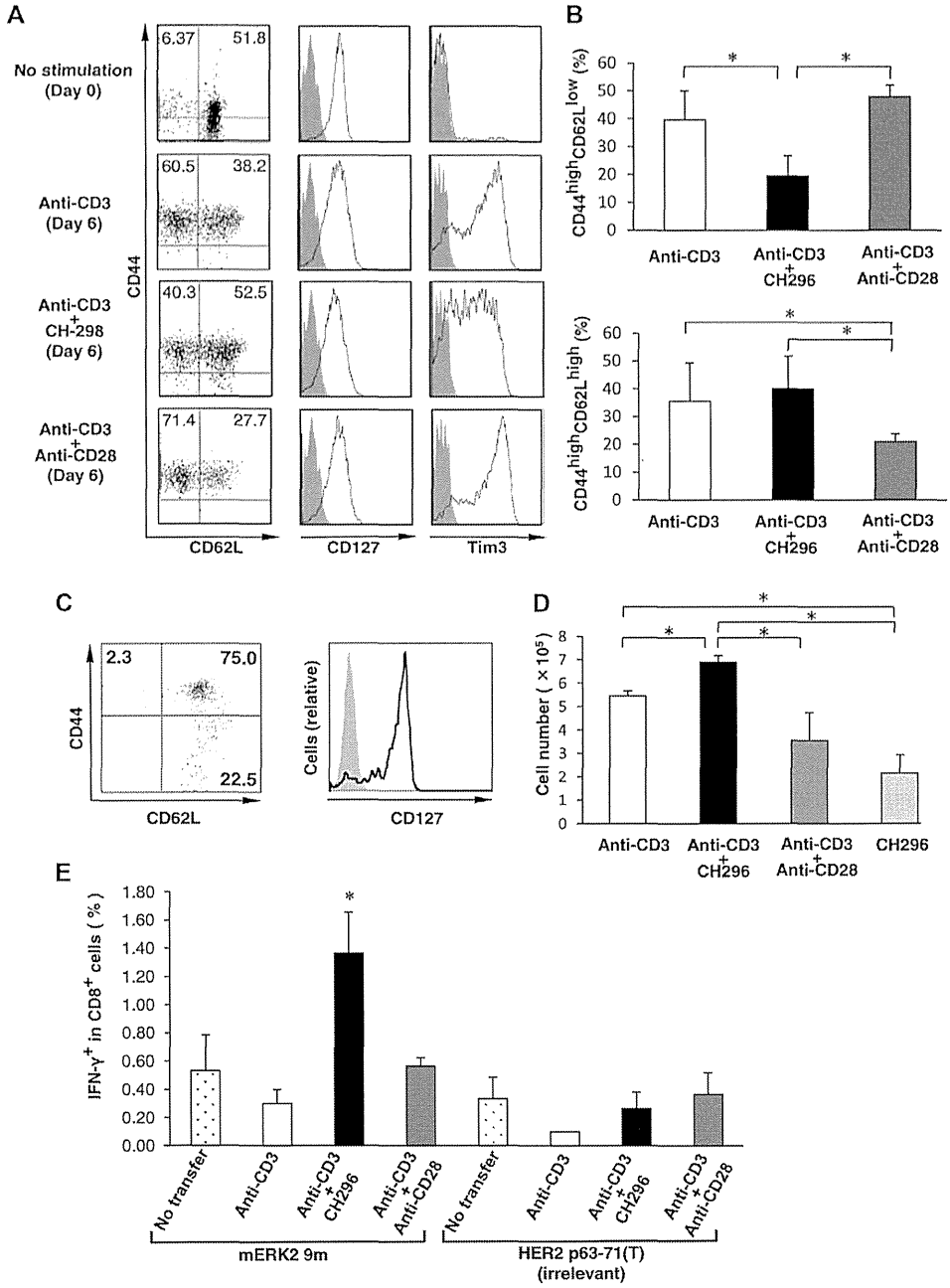

Figure 3. Transferred T cells persist longer in vivo when stimulated with CH-296 in combination with anti-CD3. A total of 1×10^6 DUC18 mouse-derived $CD8^+$ T cells stimulated with anti-CD3 mAb alone, CH-296 alone, or anti-CD3mAb in combination with CH-296 or anti-CD28 mAb for 6 days were injected intravenously into BALB/c mice ($n = 3$ per group). (A, B) Cell-surface expression of CD44, CD62L, CD127, and Tim3 in T cells prior to transfer was assessed by flow cytometry. Cells were gated using FSC-H and SSC-A to isolate small lymphocytes, followed by the gating to $CD8^+$ cells. Plots in (A) are representative of three independent experiments. (B) Data are shown as mean + SD of three independent samples. (C, D) Forty-five days after transfer, spleen cells were harvested and stained with Tg-TCR-specific tetramer and anti-CD8, anti-CD44, anti-CD62L, and anti-CD127 mAbs, then assessed by flow cytometry. (C) Cell-surface expression of CD44, CD62L, and CD127 in $CD8^+$tetramer$^+$ cells was assessed in mice receiving T cells stimulated with anti-CD3 plus CH-296. The numerical values indicate the percentage of cells among $CD8^+$tetramer$^+$ cells in the indicated quadrants. (D) Average of total cell numbers of $CD8^+$tetramer$^+$ cells in spleens of three mice was calculated from total spleen cell number and the frequency of $CD8^+$tetramer$^+$ cells determined by flow cytometry. Data show mean + SD of three samples. (E) Forty-five days after transfer of DUC18 mouse-derived $CD8^+$ T cells, spleen cells were harvested and stimulated with P1.HTR cells pulsed with mERK2-derived 9m- or control p63-peptide. The frequency of intracellular IFN-γ producing cells in $CD8^+$ fraction was assessed by flow cytometry. Data are shown as means + SD of three samples. (A–D) Results are representative of three independent experiments. (E) Results are representative of two independent experiments. Differences between groups were examined for statistical significance using Student's *t*-test. $^*p < 0.05$.

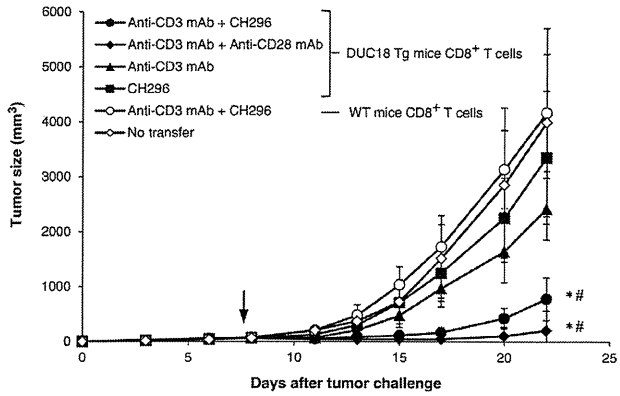

Figure 4. Priming of tumor-specific CD8$^+$ T cells by CH-296 endows T cells with the ability to inhibit tumor growth in hosts with progressing tumors. BALB/c mice ($n = 9$ per group) were inoculated subcutaneously with 1×10^6 CMS5a tumor cells on day 0. A total of 1×10^6 DUC18 mouse-derived or WT mouse-derived CD8$^+$ T cells cultured in vitro for 6 days with anti-CD3 mAb alone, CH-296 alone, or anti-CD3mAb in combination with CH-296 or anti-CD28 were injected intravenously into the lateral tail vein on day 7. Arrow indicates the time of treatment. The tumor size in each group is represented as the mean ± SD of nine samples. Results are representative of two independent experiments. Symbols indicate statistical differences in tumor size relative to mice receiving no transfer ($^*p < 0.05$) or mice receiving DUC18 CD8$^+$ T cells stimulated with anti-CD3 mAb alone ($^\#p < 0.05$). Statistical significance was assessed by one-way ANOVA with Bonferroni multiple-comparison test.

did not significantly differ among the groups. This result suggested that the tumor-infiltrating TCR-Tg T cells possessed different functional capacities among the groups, as indicated by the different recall responses (Fig. 1 and 3E).

Discussion

The primary objective of this study was to reveal the basic impact of VLA-4/5 signaling on T-cell function. In this study, we demonstrated for the first time that stimulation with a recombinant fragment of fibronectin containing the ligands for VLA-4 and -5 enhances T-cell effector multifunctionality as well as in vivo memory formation. Additionally, these findings raise the possibility that stimulation of CTLs with VLA-4 and -5 could significantly increase the efficacy of adoptive therapy against an established tumor, regardless of the requirement for several cycles of in vitro stimulation and expansion of the T cells to be used in the therapy.

Fibronectin acts in conjunction with TCR engagement to induce T-cell proliferation, which is mediated by the interaction of VLA-4 and VLA-5 with the CS1 and C domains of fibronectin [7–9]. Inhibition of apoptosis by fibronectin binding has been reported in several cell types [23–25]. Here, the acquisition of T-cell effector functionality could be attributed to binding to CH-296, which contains the CS1 and C domains. Signaling through VLA-4/5 induces tyrosine phosphorylation of proteins including FAK, phospholipase C γ, talin, paxillin, Stat1, fyn, lck, and integrin-linked kinase [3–6]. FAK plays an important role in the PI3K/Akt and Grb2/Sos/Ras/MAPK pathways [3], and also induces reconstitution of the actin cytoskeleton through activation of the small GTPase Rho [3, 26]. Consequently, FAK modulates the growth, survival, and migration of T cells. VLA-4/5 stimulation also upregulates expression of GATA-2, c-myb, and CD34 in primary hematopoietic progenitors [27]. The specific contributions of this wide range of signaling molecules to the proliferation, survival, and effector functionality of T cells remain to be determined. The significant induction of apoptosis in T cells by FAK inhibition (Fig. 2) not only indicates that this kinase is important in the antiapoptotic cascade, but also suggests the existence of other downstream signaling pathways that strongly drive cells into activation-induced cell death in the absence of FAK activation.

The increased in vivo memory formation observed in this study may depend not only on the antiapoptotic signals from VLA-4/5 but also on the localization of T cells, determined by adhesion mediated by VLA-4/5, which affects the in vivo environment including the cytokine milieu and interactions with other cell types or extracellular matrix. It would be intriguing to address the differential involvement of molecules reported to play important roles in memory formation, such as Blimp-1, mTOR, T-bet, eomesodermin, Bcl-6, and Id2, in the VLA-4/5-mediated signaling pathway [28, 29]. The importance of VLA-4/5 in the formation of T-cell memory under physiological conditions such as microbial infection or spontaneous tumor development is a topic for future investigations, although our results suggest that these integrins play a positive role in this process. Direct evidence for this question might be obtained in a future study using an animal model in which the genes encoding the corresponding integrins or their ligands are conditionally silenced.

Tissue-resident memory T (Trm) cells were recently described as a memory T-cell population that persists and patrols nonlymphoid tissues; these cells have the capacity for robust expression of cytokines and chemokines, and they serve as local sensors for previously encountered Ags and provide the protection against infection [30–32]. Cytokines such as IL-15 and TGF-β play important roles in the formation of Trm cells [33], and the molecular signature of Trm cells, including a specific set of transcription factors, chemokines, and inhibitory receptors, has been reported [34]. The mechanisms underlying the development and maintenance of Trm CD8$^+$ T cells, however, remain largely unknown. Because integrin molecules play important roles in the adhesion and homing of lymphocytes in particular tissues, it would be intriguing to address the roles of signaling through integrins, including VLA-4/5, in the formation of Trm CD8$^+$ T cells.

In this study, we attempted to translate our experimental findings into a methodology for in vitro generation of tumor-specific CTLs that have higher antitumor activity after adoptive transfer. It remains controversial whether it is advantageous to activate T cells in vitro prior to adoptive transfer. In vitro stimulation and expansion generally induce differentiation into effector cells; in contrast to naïve T cells, these cells usually exhibit reduced capacity for survival and proliferation, lose multifunctionality, and ultimately acquire the terminally differentiated senile T-cell phenotype [35, 36]. One of the potential mechanisms underlying the

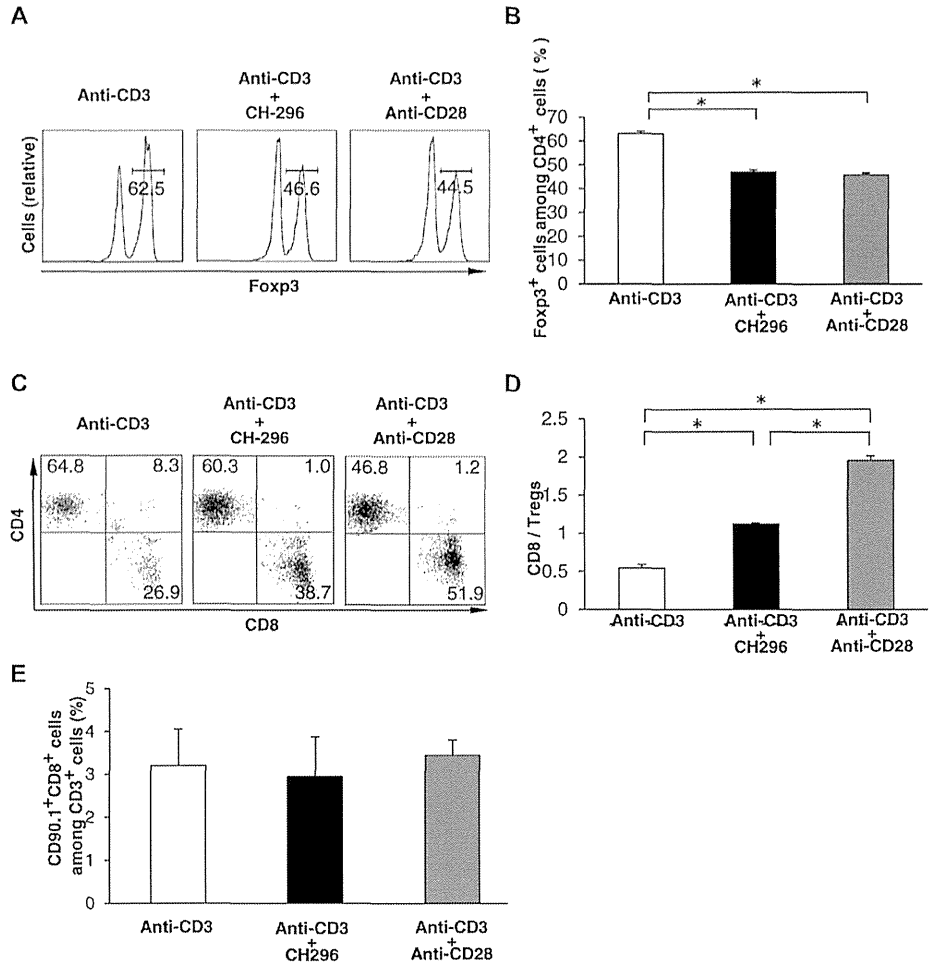

Figure 5. Tumor infiltration by $Foxp3^+CD4^+$ Treg cells decreases in mice administrated T cells stimulated with CH-296. BALB/c mice ($n = 9$ per group) were inoculated subcutaneously with 1×10^6 CMS5a tumor cells on day 0. A total of 1×10^6 DUC18 mouse-derived $CD8^+$ T cells stimulated with anti-CD3 mAb alone, or anti-CD3mAb in combination with CH-296 or anti-CD28, were injected intravenously on day 7. On day 30, lymphocytes were harvested from tumors and analyzed for their expression of CD3, CD8, CD4, and Foxp3 by flow cytometry. (A) Representative histograms of $Foxp3^+$ cells among $CD4^+$ cells. The numerical value indicates the percentage of cells within the $CD4^+$ gate in the indicated area. (B) Frequency of $Foxp3^+$ cells in $CD4^+$ cells in $CD3^+$ gate was determined by flow cytometry from data collected as in (A). Data show mean + SD of three independent samples. (C) Representative dot plots of anti-CD4 and anti-CD8 staining of tumor-infiltrating lymphocytes. The numerical value indicates the percentage of cells among $CD3^+$ cells within the indicated quadrants. (D) Ratio of $CD8^+$ cells/$Foxp3^+CD4^+$ cells among tumor-infiltrating lymphocytes was determined from data collected as in (A) and (C). (E) A total of 1×10^6 CD90.1/DUC18 mouse-derived $CD8^+$ T cells stimulated with anti-CD3 alone, or anti-CD3 in combination with CH-296 or anti-CD28, were injected intravenously on day 7. On day 30, the frequency of tumor-infiltrating $CD8^+CD90.1^+$ cells among $CD3^+$ T cells was determined by flow cytometry. Data are shown as mean + SD of three samples. (A–D) Results are representative of three independent experiments. (E) Results are representative of two independent experiments. Differences between groups were examined for statistical significance using Student's *t*-test. $^*p < 0.05$.

advantages of stimulation of $CD8^+$ T cells via VLA-4 and -5 during in vitro expansion, reported here, involves the ability of this signal to induce T-cell activation and expansion with minimal decline in survival capacity, as suggested by the inhibition of apoptosis (Fig. 2), resulting in long in vivo persistence with the memory phenotype (Fig. 3). Consistent with this finding, we previously observed that human T cells stimulated with CH-296 and anti-CD3 persisted for longer periods in nonobese diabetic/severe combined immunodeficiency mice than cells stimulated with anti-CD3 alone [10], although the xenogeneic conditions made a precise interpretation difficult.

This study revealed the difference between VLA-4/5 and CD28 signaling with respect to the quality of co-stimulation of T cells. Murine T cells stimulated with CD3/CD28 acquired higher proliferation capacity (Supporting Information Fig. 3), which could result in larger cell numbers following adoptive transfer. These cells mainly exhibited well-differentiated effector phenotypes (Fig. 3A and B) and transient but direct antitumor effector functions (Supporting Information Fig. 2). On the other hand, CD3/CH-296 signals provided relatively mild stimulation, and induced less T-cell proliferation than CD3/CD28 signals. However, T cells stimulated with CD3/CH-296 exhibited a high frequency of

the central/effector memory phenotype (Fig. 3A and B) and high multifunctionality in response to recall stimulation (Supporting Information Fig. 1), as well as higher capacity to form memory cells (Fig. 3). Therefore, the signals mediated by VLA-4/5 and CD28 had different advantages and disadvantages with respect to the generation of T cells for adoptive transfer immunotherapy, resulting in comparable inhibition of tumor growth by both signals under our experimental conditions (Fig. 4).

In initial trials in which tumor-reactive T-cell lines or clones were administered to cancer patients, both clinical response and persistence of infused cells have been limited [37, 38]. Recent studies suggest that these disappointing outcomes might be related to two major obstacles: the immunosuppressive environment within tumor-bearing hosts [39, 40], and the reduced quality of T cells that have been expanded by long-term in vitro culture [15, 36]. To overcome these obstacles, clinical protocols that incorporate pretreatment of patients with lymphodepleting chemotherapy and/or irradiation have been proposed [41–43]. Combination of these maneuvers with high-dose interleukin-2 (IL-2) administration has resulted in an objective response rate of ~50% or more in clinical trials of patients with advanced metastatic melanoma [11, 41, 42]. However, these pretreatments are often associated with significant toxicity in humans, including potentially life-threatening hematologic toxicities associated with opportunistic infections, as well as severe nonhematologic toxicities [41, 42]. Therefore, it is important to establish strategies for improving the antitumor effect of adoptive T-cell therapy that minimize the requirement for pretreatments that risk adverse side effects.

The importance of T-cell multifunctionality has been reported in multiple animal infection models, as well as in humans infected with human immunodeficiency virus, cytomegalovirus, hepatitis B virus, or tuberculosis [36, 44]. We previously described the importance of effector T-cell multifunctionality in the antitumor immune response [17–19], consistent with clinical observations reported by other groups [45, 46]. The differences in the qualities of T-cell responses defined by different combinations of functions remain largely unknown. Also unclear are the mechanisms underpinning the physiological relevance of multifunctionality as a sensitive biomarker of the immunological control of diseases. To approach these longstanding unresolved questions, it will be important to address the molecular basis and genetic/epigenetic control of T-cell multifunctionality in future studies.

In summary, our data suggest that the incorporation of stimulation with VLA-4 and -5 into the conditions for the initial in vitro expansion of tumor-reactive T cells can improve $CD8^+$ T-cell multifunctionality and memory formation. These findings were useful in in vitro stimulation and expansion of tumor-specific CTLs for an adoptive immunotherapy model. The information presented here sheds new light on the programs in T cells that control their functions, phenotypes, and ultimate fates. Our findings may also be useful in the future development of clinical protocols for adoptive T-cell immunotherapy that are both efficacious and minimally toxic.

Materials and methods

Human samples

PBMCs were isolated by Ficoll/Conray density-gradient centrifugation from blood of healthy donors, all of whom gave their written informed consent. The experimental protocols were approved by the Ethics Review Committees of the Mie University Graduate School of Medicine and Takara Bio Inc.

Mice

Studies were conducted on 7- to 10-week-old female BALB/c mice (CLEA Japan, Osaka, Japan) or DUC18 mice [20] transgenic for TCR reactive to K^d-restricted 136–144 peptide of mutated mitogen-activated protein kinase (extracellular signal-regulated kinase 2, mERK2) [47]. BALB/c-Thy1.1 (CD90.1) congenic mice [48] were generously provided by Dr. Shimon Sakaguchi (Immunology Frontier Research Center, Osaka University), and crossed with DUC18 mice in our laboratory. Mice were maintained at the Animal Center of the Mie University Graduate School of Medicine. The experimental protocol was approved by the Ethics Review Committee for Animal Experimentation of the Mie University Graduate School of Medicine.

Cell lines

CMS5 is a methylcholanthrene-induced sarcoma cell line of BALB/c origin expressing mERK2 [47]. P1.HTR is a subline of mastocytoma P815 of DBA/2 origin [49]. The CMS5a and P1.HTR cell lines were kindly provided by the late Dr. L.J. Old (Ludwig Institute for Cancer Research, New York Brunch, Memorial Sloan-Kettering Cancer Center, New York) in 1996. Their identities were confirmed by immunological tests, tumorigenicity, and Ag-presenting function once a year. These cell lines were cultured in RPMI-1640 (Sigma-Aldrich) medium supplemented with 10% heat-inactivated FCS (Sigma-Aldrich), 55 μM 2-ME, 100 U/mL penicillin, 100 mg/mL streptomycin, and 0.2 mg/mL glutamine.

Stimulation of lymphocytes

Human PBMCs were stimulated with or without CH-296 (RetroNectin; precoated 10 μg/well; Takara Bio) in a 12-well plate (5×10^5 cells/well) in combination with anti-CD3 mAb (precoated 2 μg/well) in GT-T503 medium (Takara Bio) supplemented with 0.2% human serum albumin (Sigma-Aldrich), 5 mg/mL fungizone (Bristol-Myers Squibb), 0.6% autologous plasma, and 40 IU/mL recombinant human IL-2 (Takeda Co., Tokyo, Japan). Mouse spleen cells were seeded in 6-well plates at a density of

1×10^6 cells/well in a total volume of 5 mL, and stimulated with or without CH-296 (30 μg/well) or anti-CD28 (1 μg/mL) in combination with anti-CD3 mAb (6 μg/well) in RPMI-1640 (Sigma-Aldrich) medium supplemented with 10% heat-inactivated FCS (Sigma-Aldrich), 55 μM 2-ME, 100 U/mL penicillin, 100 mg/mL streptomycin, 0.2 mg/mL glutamine, and 20 IU/mL recombinant human IL-2. After harvest on day 3, the cells were seeded on uncoated wells. They were then maintained until day 6 without further stimulation. All cells were grown at 37°C in a 5% CO_2 humidified incubator.

Abs and reagents

For flow-cytometric analysis, the following Abs were used: PerCP-Cy5.5-conjugated anti-mouse CD8 (53–6.7), FITC-conjugated anti-mouse TCRVβ8.3 (1B3.3), FITC-conjugated anti-human IFN-γ (4S.B3), allophycocyanin -Cy7-conjugated anti-mouse TNF (MP6-XT22), allophycocyanin-conjugated anti-human CD107a (H4A3), phycoerythrin (PE)-Cy7-conjugated anti-mouse CD107a (1D4B), PE-conjugated anti-mouse CD137 (1AH2), PE-conjugated anti-mouse CD27 (LG.3A10), PE-conjugated anti-mouse CD28 (37.51), and V500-conjugated anti-mouse CD44 (IM7). Allophycocyanin-conjugated Annexin V, 7-AAD, and Annexin V binding buffer were purchased from BD Biosciences (San Jose, CA, USA). Allophycocyanin-Cy7-conjugated anti-human CD8a (RPA-T8) was purchased from Biolegend (San Diego, CA, USA). Allophycocyanin-conjugated anti-mouse IFN-γ (XMG1.2), Pe-Cy7-conjugated anti-human TNF (MAb11), PE-conjugated anti-mouse Foxp3, allophycocyanin-conjugated anti-mouse CD127 (A7R34), and eFluor 450-conjugated anti-mouse CD62L were purchased from eBioscience (San Diego, CA, USA). PE-conjugated anti-mouse VLA-4 (PS/2) and FITC-conjugated anti-mouse VLA-5 (5H 10–27) mAbs were purchased from Beckman Coulter (Brea, CA, USA). For blocking or stimulation, the following Abs and isotype controls were used: anti-mouse VLA-4 (PS/2), anti-mouse VLA-5 (5H10-7) mAbs, and Rat IgG2bκ (KLH/G2a-1-1), all purchased from Beckman Coulter. Anti-human CD3 (OKT3), Rat IgG2aκ (eBR2a), and anti-mouse CD28 (37.51) were purchased from eBioscience. Anti-mouse CD3 (145-2C11) was purchased from BD Biosciences. CFSE was purchased from Molecular Probes (Eugene, OR, USA). Synthetic mERK2 9m peptide QYIHSANVL [47] and HER2 oncoprotein-derived $HER2p_{63-71}$ (T) peptide TYLPTHASL [50] have been previously described, and were purchased from Qiagen. PF-573228, a specific inhibitor of FAK phosphorylation, was purchased from Sigma-Aldrich. PE-conjugated 9m-K^d tetramer was kindly provided by Dr. P. Guilliaume and Dr. I. Luescher (The Ludwig Institute Core Facility, Lausanne, Switzerland).

Intracellular cytokine staining

Human PBMCs were stimulated on plates coated with anti-CD3 (1 or 5 μg/mL) in the presence of 0.1 mg/mL allophycocyanin-conjugated anti-CD107a. We then incubated these samples for an additional 5 h after the addition of 1 μL/mL GolgiStop (BD Biosciences). Samples were washed with RPMI1640, and then stained with allophycocyanin-Cy7-conjugated anti-CD8a. After permeabilization and fixation using the Cytofix/Cytoperm Kit (BD Biosciences), cells were stained intracellularly with FITC-conjugated anti-IFN-γ and PE-Cy7-conjugated anti-TNF. Mouse spleen cells were stimulated according to a similar protocol, except that P1.HTR cells pulsed with 1 μM 9m peptide or control $HER2_{63-71}$ peptide (an irrelevant peptide with H-$2K^b$-binding activity [50]) were used as stimulator cells in place of anti-CD3 stimulation, and the following reagents were used: PE-Cy7-conjugated anti-mouse CD107a, GolgiPlug (BD Biosciences), PerCP-Cy5.5-conjugated anti-mouse CD8, FITC-conjugated anti-TCRVβ8.3, allophycocyanin-conjugated anti-mouse IFN-γ, and allophycocyanin-Cy7-conjugated anti-mouse TNF.

Flow-cytometry analysis

Flow-cytometric acquisition was performed on a FACSCantoII (BD Biosciences). Analysis was performed using the FlowJo software (Tree Star).

Tumor challenge

BALB/c mice ($n = 9$ per group) were inoculated subcutaneously in the right hind flank with 0.2 mL PBS containing 1×10^6 CMS5a cells. After inoculation, the mice were monitored three times per week with digital calipers. Evaluations of tumor size were performed according to the following formula: volume = major axis × (minor axis)^2/2. Mice were sacrificed according to institutional guidelines when the longest diameter of the tumor reached 20 mm. Tumor-infiltrating lymphocytes were obtained as described previously [17].

Adoptive cell transfer

Stimulated spleen cells were harvested on day 6 of in vitro culture. After three washes in PBS, spleen cells containing 1×10^6 $CD8^+$ cells were suspended in 0.2 mL of PBS and injected intravenously into a lateral tail vein. Before injection, we checked the ratio of $CD8^+$ events in each group by flow-cytometric analysis, in order to adjust the number of $CD8^+$ cells to be injected.

Cytotoxicity assay

The ability of human lymphocytes to lyse targets was measured using a calcein-AM (Dojindo) release assay as described previously [51]. Cytotoxicity of murine T cells was evaluated by a Cr-release assay as described previously [47].